UCRL-53476
Distribution Category UC-70

UCRL--53476

DE84 015922

Thermal Conductivity and Diffusivity of Permian Basin Bedded Salt at Elevated Pressure and Temperature

W. B. Durham

C. O. Boro

J. M. Beiriger

D. N. Montan

Manuscript date: October 1983

LAWRENCE LIVERMORE NATIONAL LABORATORY
University of California • Livermore, California • 94550

Available from: National Technical Information Service • U.S. Department of Commerce
5285 Port Royal Road • Springfield, VA 22161 • $8.50 per copy • (Microfiche $4.50)

Contents

Thermal Conductivity and Diffusivity of Permian Basin Bedded Salt at Elevated Pressure and Temperature

Abstract

Measurements of thermal conductivity and diffusivity were made on five core samples of bedded rock salt from the Permian Basin in Texas to determine its suitability as an underground nuclear waste repository. The sample size was 100 mm in diameter by 250 mm in length. Measurements were conducted under confining pressures ranging from 3.8 to 31.0 MPa and temperatures from room temperature to 473 K. Conductivity showed no dependence on confining pressure but evidenced a monotonic, negative temperature dependence. Four of the five samples showed conductivities clustered in a range of 5.6 ± 0.5 W/m·K at room temperature, falling to 3.6 ± 0.3 W/m·K at 473 K. These values are approximately 20% below those for pure halite, reflecting perhaps the 5 to 20%-nonhalite component of the samples. Diffusivity also showed a monotonic, negative temperature dependence, with four of the five samples clustered in a range of 2.7 ± 0.4 × 10^{-6} m^2/s at room temperature, and 1.5 ± 0.3 × 10^{-6} m^2/s at 473 K, all roughly 33% below the values for pure halite. One sample showed an unusually high conductivity (it also had the highest diffusivity), about 20% higher than the others; and one sample showed an unusually low diffusivity (it also had the lowest conductivity), roughly a factor of 2 lower than the others.

Introduction

Rock salt formations are among the leading contenders as sites for underground nuclear waste repositories, and interest in their viabilty as waste repositories has clearly gone from general overview to focused site specific attention. Before a respository is constructed in salt formations, it is necessary to predict with the best possible accuracy how the repository will respond to the heat from the nuclear waste load. Such predictions depend on an accurate knowledge of the pertinent physical properties of the repository medium under in situ physical and chemical conditions.

We report here measurements of two such physical properties, thermal conductivity and thermal diffusivity, made on five core samples from the Permian Basin salt formations in the Texas panhandle, one of the sites under consideration in the United States. Conductivity, which characterizes heat energy transport in the steady-state situation, and diffusivity, which characterizes transport in the transient situation, must be known to predict temperature profiles in future repositories.

Sample and Standard Reference Material

Sample rock material was cored from the Cycle 4 and Cycle 5 bedded salt formations in the Permian Basin in Deaf Smith County, Texas panhandle. We measured five salt samples (Table 1): two from each of the two horizons in the G. Friemel #1 and Detten #1 wells, and a repeat sample from the lower horizon in the Detten #1 well. Petrographic analyses are available for all

Table 1. Description of sample material and summary of the petrographic analyses.

Sample	Well	Depth (ft)	Composition (%)			Distance to nearest petrographic analysis (ft)
			Halite	Clay	Anhydrite	
TP7	Detten #1	2454-2455	78-85	6-12	8-9	5
TP8	G. Friemel #1	2523-2524	93-94	2-5	1-3	10
TP9	G. Friemel #1	2308-2309	89	2	8	1.5
TP10	Detten #1	2654-2655	–[a]	–[a]	–[a]	~180
TP11	Detten #1	2655-2656	–[a]	–[a]	–[a]	~180

[a] Analysis not available.

horizons except the lower one at Detten #1 (Dixon, 1982; Fukui, 1982) and are summarized in Table 1. The material varies between 78 and 94% halite with the balance being primarily a mix of clay minerals and anhydrite. The grain size of the halite ranges from medium (<10 mm) to coarse (~50 mm).

Our reference standard is made from Pyroceram Code 9606, a microcrystalline ceramic material manufactured by Corning Glass Works (CGW), Corning, N.Y. The material was created during CGW's slabbing operation at the end of the single 1982 production run. Pyroceram 9606 is a particularly uniform and chemically stable material that the National Bureau of Standards considered nearly 20 years ago as a standard reference material for thermal conductivity and diffusivity (Flynn et al., 1964). Flynn et al. give a detailed description of the manufacturing process.

In this study, we take the unconfined (i.e., confining pressure = 0.1 MPa) diffusivity of Pyroceram 9606 to be amongst the curves of Plummer et al. (1962), Flieger (1963), and Rudkin (1963), as shown in Fig. 1; for the unconfined conductivity,

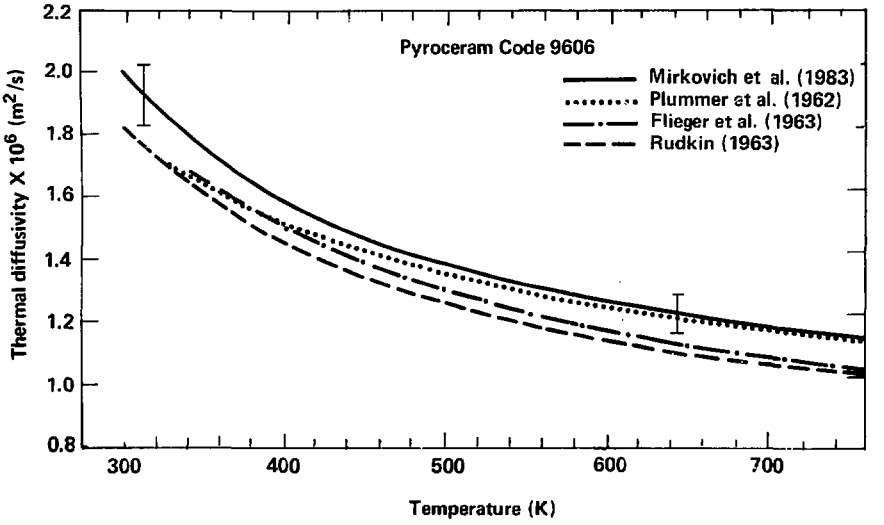

Figure 1. Thermal diffusivity of Pyroceram Code 9606. The curves from 1962 and 1963 are the standard reference values. More recent data from Mirkovich and coworkers are also shown. The error bars encompass the scatter of the Mirkovich et al. data.

we take the values of Touloukian et al. (1970), as shown in Fig. 2. Pyroceram 9606 is essentially 100% dense, i.e., it has zero porosity; therefore, its physical properties would not be expected to exhibit any extrinsic (crack- and pore-related) pressure dependence. Since Pyroceram 9606 has a bulk modulus in the range of 80 GPa, it should not show any measureable intrinsic pressure effects until well outside the 0–30-MPa pressure range covered in this study. Mirkovich et al. (1983) confirmed the independence of thermal diffusivity and pressure between 0.1 and 200 MPa.

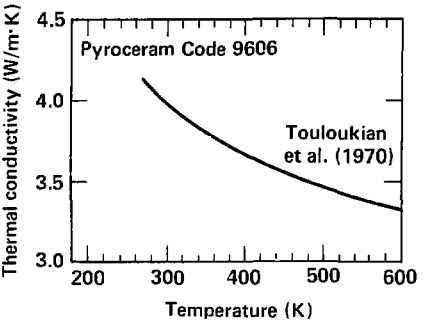

Figure 2. Recommended values of thermal conductivity vs temperature for Pyroceram Code 9606 (Touloukian et al., 1970).

Sample and Standard Preparation

Salt cores were supplied in short segments approximately 300 mm long and 105 mm in diameter. As received, each segment was wrapped in plastic, cushioned inside a stiff plastic tube, the ends of which were capped and sealed with duct tape, and packaged individually. A notation on each package indicated core location and depth (Table 1). With the exception of the core used for the first sample, TP7 (our sample notation), we did not open the containers until shortly before preparation began; TP7 was opened several days in advance of its preparation as we developed the jacketing procedure outlined below. The elapsed time from opening the packing containers to complete sample encapsulation was typically 2–3 wk. During extended periods of nonhandling, such as overnight and weekends, we put the opened sample material in unsealed plastic bags.

At the Lawrence Livermore National Laboratory (LLNL), Livermore, Calif., we machined the samples to thick-walled cylinders 254 mm long with 21- and 102-mm inner and outer diameters. The cyclinders were encapsulated in metallic jackets, as shown in Fig. 3, to exclude the high pressure confining medium (argon gas) from the pores and cracks of the salt to retain the validity of the simulation of lithostatic pressure.

As supplied, the salt core had an irregular outer diameter that occasionally fell below the 102-mm level required for the sample assembly. We filled the low-lying pockets by isostatically pressing a lead jacket onto the salt sample prior to the first machining step. The assembly was then machined down to a smooth 102-mm outer diameter, effectively removing most of the initial lead jacket. It is significant to note, for reasons discussed below, that the isostatic pressure in this prejacketing step was 10 to 12 MPa and was maintained for several minutes.

Next, we drilled the central hole and faced the ends of the salt. Note that jacketing included the outer and inner diameter and the ends of the salt sample. We used an outer lead jacket 3 mm thick (at its minimum) and a copper inner jacket over 1 mm thick to avoid failure of a jacket by pressing into a local void. The measurement technique (described below) required that the inner jacket have a high thermal conductance radially and a low conductance axially; hence, the inner jacket was made of copper and as thin as possible, and all but 0.25 mm of its full wall thickness was interrupted at either end with a 20-mm long sleeve of pyrophylite, a machinable, low conductivity material.

We placed six sheathed 1.5-mm diameter Type J (iron-constantan) thermocouples at six logarithmically spaced radii (Table 2) in the central radial plane of a sample. The thermocouples were distributed azimuthally to minimize thermal shadowing effects of one upon the other. They

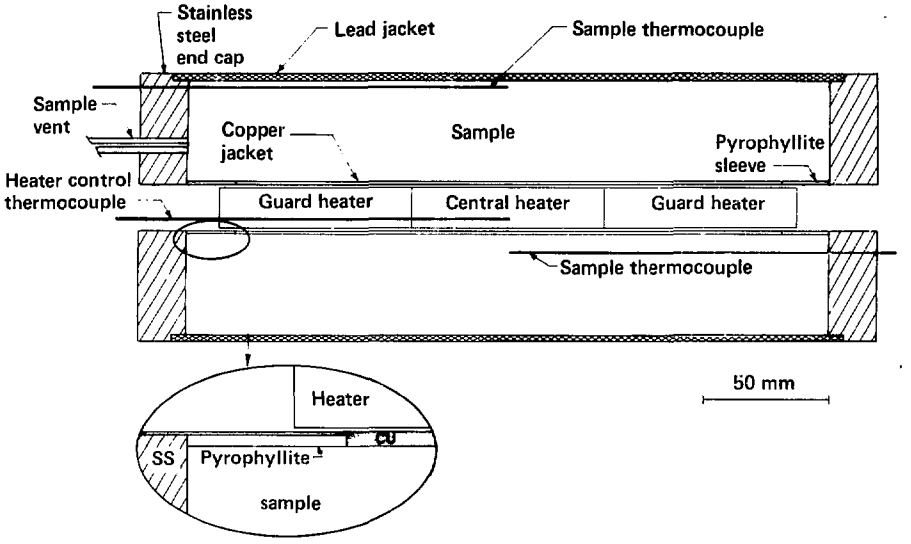

Figure 3. Scale drawing of the sample assembly. Only two of the six sample thermocouples are shown.

were introduced axially through the ends of the sample assembly, three from each end, in close fitting holes drilled in the salt. Thermocouple sheaths were brazed to the sample end caps to retain the pressure seal around the sample. Through one end cap, we inserted a sample vent of high pressure tubing that ultimately passed through the pressure vessel to the outside. The vent maintained pore pressure at 0.1 MPa and also served as a leak detecting device.

We received the Pyroceram 9606 reference standard from CGW in its final form; it lacked only the six thermocouple holes, which were cored at LLNL prior to jacketing. The standard was fabricated from six discs of approximately equal thickness that were cemented together with Corning Code 7574 devitrifying solder glass. The joints between the discs spanned less than 0.25 mm and were barely visible. CGW could not guarantee that the joints were free of air pockets; but since the joints lay in the plane normal to the axis, and heat flow was primarily radial, we anticipated no problems. The numerical simulation of the experiment, discussed in Appendix A, demonstrated that altering the conductance of the joints from infinite to zero has an effect that is barely perceptible. We jacketed the reference standard in precisely the same manner as the salt samples.

Table 2. Thermocouple position error for Sample TP9.

Nominal radius (mm)	TP9 radius (±0.25 mm)	Position error (mm)
16.84	16.40	−0.4
20.37	21.65	+1.3
25.30	24.95	−0.4
31.04	32.00	+1.0
38.05	38.55	+0.5
46.69	46.45	−0.2

Experimental Design

Measurement Technique

The measurement technique is a refined version of that described by Abey et al. (1982) and Durham and Abey (1983). The sample assembly (Fig. 3) resides inside an externally heated pressure vessel wherein pressurized argon gas and power supplied to the external heaters provide the hydrostatic pressure (P) and temperature (T) to simulate appropriate ambient conditions in the earth. The vessel has a design range to P = 200 MPa (simulating burial depths of 6 to 8 km) and T = 773 K.

The three low-power internal heaters shown in Fig. 3 provide a temperature gradient in the sample that is needed to measure thermal conductivity and diffusivity. The six sample thermocouples measure the gradient. Clock time (needed for the diffusivity measurement) and power to each of the three core heaters are also measured. Voltage taps for the power measurements are taken at the point of emergence of the heater leads from the axial hole in the sample. A host of thermocouples within and around the sample assembly and pressure vessel is used for diagnostic purposes and to control the internal and external heaters.

The diffusivity measurement technique is identical to that described by Abey et al. (1982). We allowed the sample to reach thermal equilibrium at the desired (P,T) conditions, powered up the three internal heaters to near full capacity, and measured the temperature as a function of time (t) and radius (r) in the sample. We then used an iterative technique to fit the $T(r,t)$ data to the cylindrical diffusivity equation

$$\frac{dT}{dt} = \kappa\left(\frac{1}{r}\frac{dT}{dr} + \frac{d^2T}{dr^2}\right) \quad , \tag{1}$$

where κ = thermal diffusivity.

Thermal conductivity λ is measured by the infinite line source method wherein $T(r)$ is related to the conductivity and power per unit length of the line source q by

$$T(r) = \frac{q}{2\pi\lambda}\log_e r \quad . \tag{2}$$

See, for instance, Schneider (1955) for a derivation of Eq. (2). We refined the measurement technique to allow determination of λ in situations where Eq. (2) is not strictly applicable. The refinement was necessitated by the extreme experimental difficulty in identifying the conditions under which Eq. (2) does strictly apply. The technique is outlined in Appendix A.

Figure 4 schematically shows the sequence of (P,T) conditions under which the measurements were made. The sequence we chose was based on utility and a desire to minimize thermally induced damage. Rocks generally suffer permanent damage in the form of microfracturing as temperature increases at low pressures (rock salt, because of its nearly isotropic character, may be an important exception); consequently, we experimented first with lower temperatures and higher pressures. All pressures were sampled in sequence at a given temperature, simply because the system can change pressure much more rapidly than it can change temperature. Note that heating was always at 31 MPa, the highest pressure used. All five salt samples followed the identical path. We investigated neither the effects of cycling nor the effects of following a different path in (P,T) space. The path for the reference standard was the same, except a second excursion to 338 K was added after the measurement at 408 K; the measurements at room temperature were taken last.

Measurement Error

The measurement error and random noise of the basic signals follow.

The pressure transducer was calibrated between runs TP8 and TP9 at the LLNL Standards and Calibration Laboratory. The transducer showed no significant shift in its gain or zero since its purchase four years ago. Periodic relative calibration against any of several gas regulator gauges was done for pressures up to 12 MPa to diagnose potential problems; none was ever detected. The bandwidth on the P setpoint was approximately $\pm 2\%$ at $P > 3.8$ MPa and $\pm 8\%$ at P = 3.8 MPa. This quasi-random error far outweighed the measurement error.

Temperatures in the sample and experimental assembly were measured with a large number of Type K and Type J thermocouples of stated accuracy $\pm$ 1-2 K. Relative temperatures of the sample thermocouples were checked at each ambient

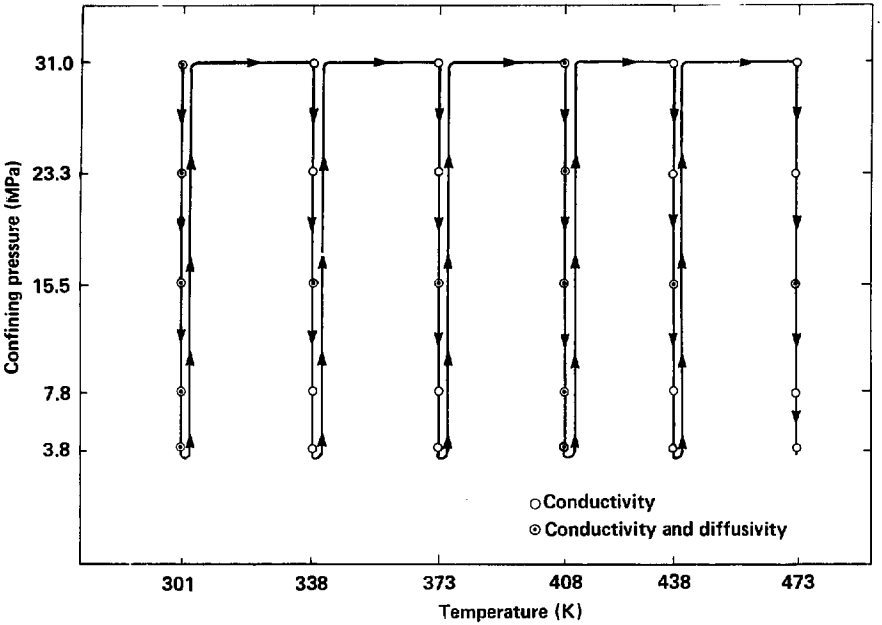

Figure 4. Path followed in pressure-temperature space for the measurements. Note that conductivity was measured at each stopping point; diffusivity was measured only at some of the stopping points.

(P,T) condition in each run as described in Appendix B and appropriate corrections were applied for each measurement. Between corrections, we never detected a drift in relative readings beyond the precision of the measurement device (±0.1 K). Note that since a temperature gradient existed in the sample during a conductivity test, and a dynamic gradient existed during a diffusivity test, a strictly ambient T condition did not exist. The "ambient" T for the conductivity measurement was arbitrarily taken to be that of the fifth (of six) most outward sample thermocouple; for the diffusivity measurement, it was taken to be the set point temperature of the outer heaters. The accuracy of the "ambient" T was, therefore, about ±3 K in both tests.

The measurement device was checked periodically with a voltage source (as was done with the thermocouples). The shunt resistances used for current measurement have a stated accuracy of ±1% and were assumed not to drift. The measurement technique of comparison against a standard was designed to calibrate out inaccuracies in the power measurement.

Results

We measured conductivity at all six temperatures at all five pressures (Fig. 4) on samples TP8–TP11 and on the reference standard. Measurements at 7.8 and 23.3 MPa were eliminated from the test matrix of TP7. We measured diffusivity at roughly half the conductivity points in (P,T) space as indicated in Fig. 4; we measured it at all five pressures (or three, in the case of TP7) at 301 K and 408 K and at all six temperatures at 15.5 MPa. Figure 5 plots the final results for conductivity and Fig. 6 plots the final results for diffusivity.

Conductivity measurements were referenced to the known values for Pyroceram, that is, measurements on the salt were adjusted on the basis of the difference between the measured and expected values for Pyroceram. The calculation is described in detail in Appendix A. Thermal diffusivity measurements on the Pyroceram 9606 reference standard (Fig. 6) gave values approximately 5% higher than expected at 300 and 340 K and approximately 5% lower than expected at 400 K and above. Since the scatter in our measurements on the Pyroceram was almost ±5%, we did not feel that a correction to the salt measurement was justified.

Approximately half a million individual data (times, temperatures, pressures, currents, voltages) were gathered, of which approximately 60% fell into the category of diagnostic and control. The remaining 200,000 data actually used to determine conductivity and diffusivity are still prohibitively numerous to include here. Instead, we present samples of the records in Appendices B and C. The reduced data related to conductivity [power, power ratio (P.R.), $\lambda_{apparent}$], which eventually lead to the plots in Fig. 5, form a table of approximately 540 lines. Again, we present representative extracts (Tables 3 and 4). The data reduction process for thermal diffusivity leads directly to the (P,T,κ) relationships shown in Fig. 6. All data remain stored on magnetic disc, in duplicate, and are easily accessible upon request.

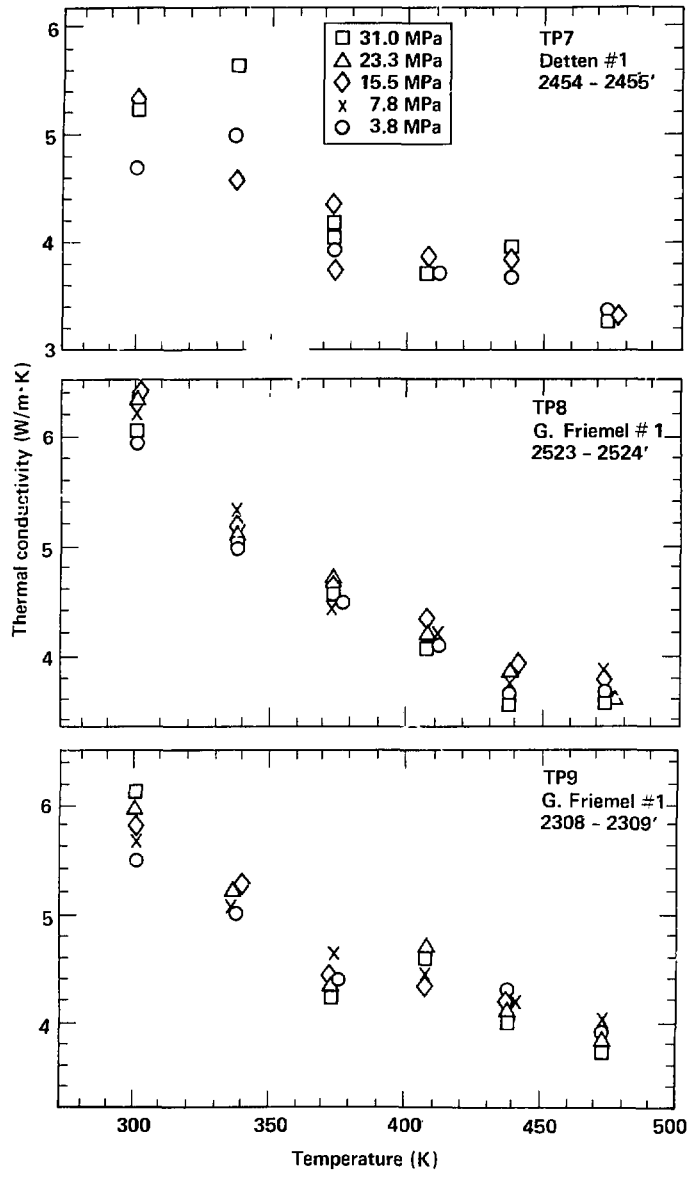

Figure 5. Results of thermal conductivity vs temperature and pressure for five rock salt samples and the reference standard. The curve through the data for the Pyroceram 9606 is taken from Fig. 2.

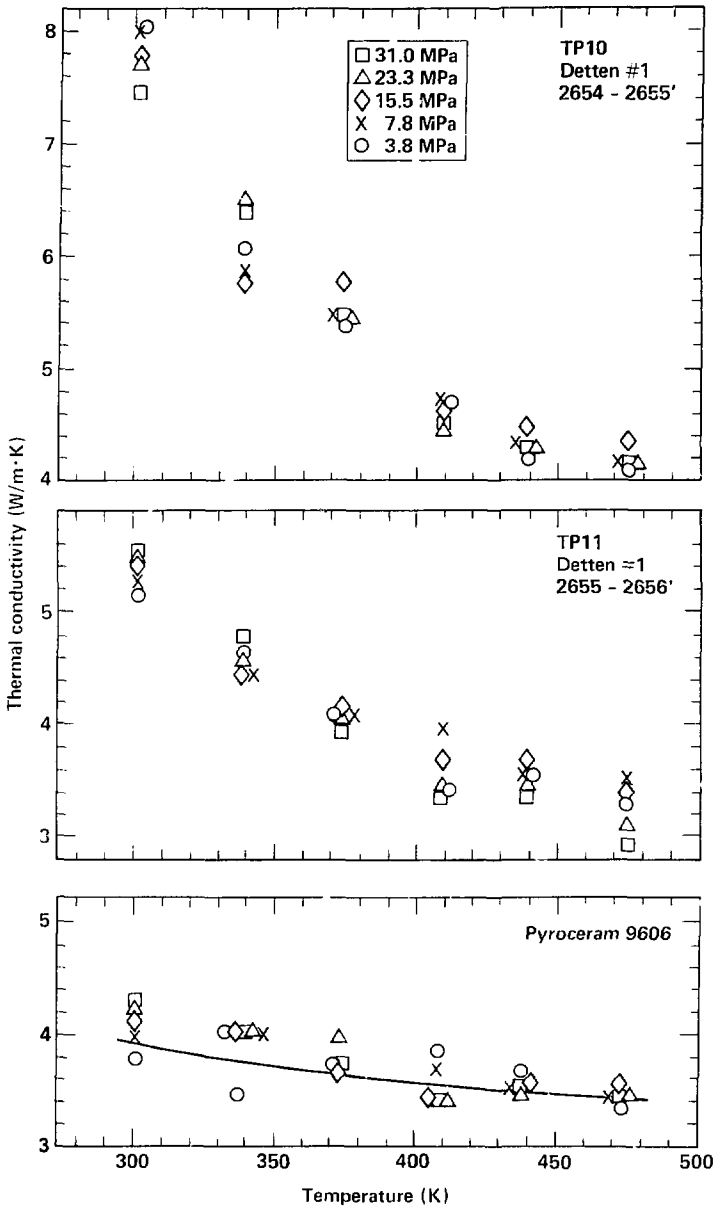

Figure 5. Contined.

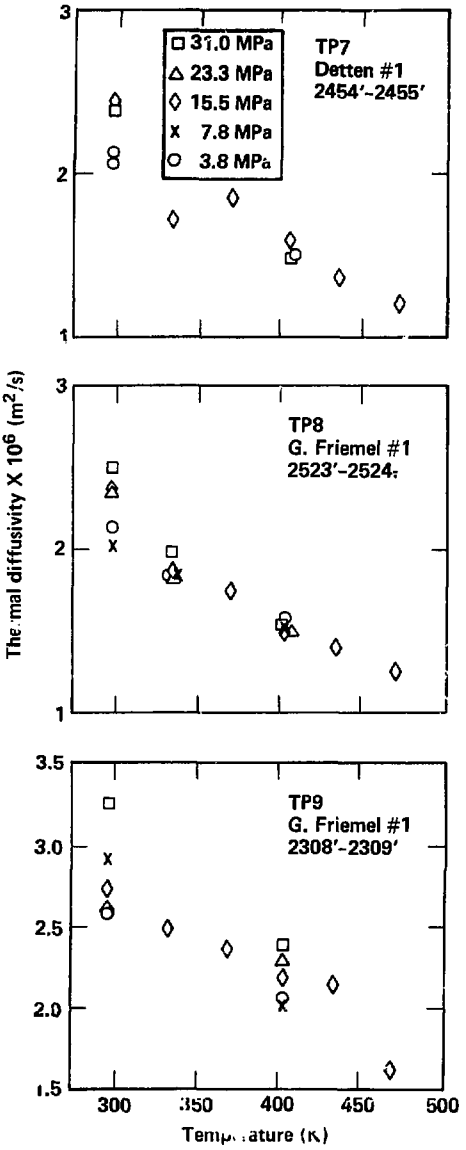

Figure 6. Results of thermal diffusivity vs temperature and pressure for five rock salt samples and the reference standard. The curve through the data for the Pyroceram 9606 is taken from Fig. 1.

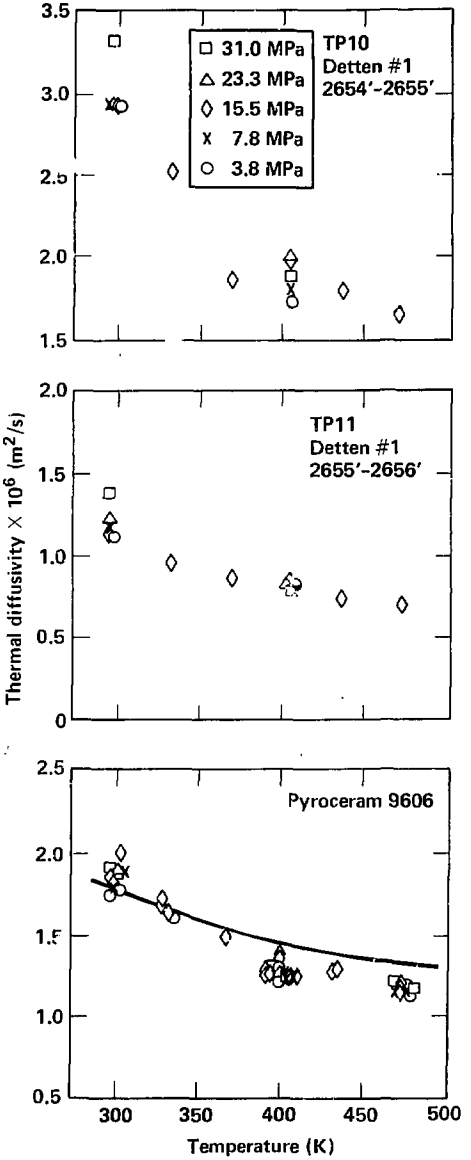

Figure 6. Continued.

Table 3. Examples of the reduced data.

Sample	P (MPa)	T_{rock} (°C)	T_{htr} (°C)	P.R.	$\lambda_{apparent}$ (W/m·K)	Power (W)	λ_{actual}	$\overline{\lambda}_{actual}$
TP7	31.0	100	115.0	1.0	4.28	11.33	4.20	
	31.0	100	114.8	1.2	3.66	9.90	4.01	4.03
	31.0	100	114.6	1.4	3.21	8.86	3.89	
	15.5	100	114.6	1.4	2.94	7.54	3.76	
	15.5	100	114.8	1.2	3.25	8.42	3.75	3.76
	15.5	100	115.0	1.0	3.64	9.47	3.75	
	3.8	100	115.0	1.0	3.81	8.87	3.94	
	3.8	100	114.8	1.2	3.36	7.78	3.89	3.93
	3.8	100	114.6	1.4	3.09	7.00	3.97	
TP8	31.0	100	116.6	1.4	3.69	9.03	4.49	
	31.0	100	116.8	1.2	4.07	10 05	4.48	4.47
	31.0	100	117.0	1.0	4.52	11.22	4.44	
	15.5	100	116.6	1.4	3.51	7.67	4.52	
	15.5	100	116.8	1.2	3.91	8.61	4.55	4.51
	15.5	100	117.0	1.0	4.29	9.53	4.46	
	3.8	100	116.6	1.4	3.45	6.71	4.45	
	3.8	100	116.8	1.2	3.81	7.45	4.44	4.45
	3.8	100	117.0	1.0	4.29	8.38	4.47	
TP9	31.0	100	115.0	1.0	4.38	10.80	4.30	
	31.0	100	114.8	1.2	3.90	9.58	4.28	4.28
	31.0	100	114.6	1.4	3.50	8.57	4.25	
	15.5	100	115.0	1.0	4.30	9.26	4.47	
	15.5	100	114.8	1.2	3.80	8.17	4.42	4.43
	15.5	100	114.6	1.4	3.42	7.34	4.40	
	3.8	100	114.6	1.4	3.34	6.72	4.30	
	3.8	100	114.8	1.2	3.77	7.49	4.39	4.40
	3.8	100	115.0	1.0	4.32	8.44	4.50	
TP10	31.0	100	115.0	1.0	5.47	9.87	5.43	
	31.0	100	114.8	1.2	4.94	8.79	5.47	5.43
	31.0	100	114.6	1.4	4.40	7.89	5.38	
	15.5	100	115.0	1.0	5.27	8.43	5.54	
	15.5	100	114.8	1.2	4.95	7.53	5.82	5.76
	15.5	100	114.6	1.4	4.55	6.75	5.91	
	3.8	100	115.0	1.0	5.01	7.42	5.26	
	3.8	100	114.8	1.2	4.61	6.52	5.41	5.40
	3.8	100	114.6	1.4	4.25	5.91	5.52	
TP11	31.0	100	115.0	1.0	4.04	9.38	3.95	
	31.0	100	114.8	1.2	3.59	8.36	3.93	3.94
	31.0	100	114.6	1.4	3.25	7.50	3.94	
	15.5	100	114.6	1.4	3.20	6.46	4.11	
	15.5	100	114.8	1.2	3.56	7.20	4.13	4.13
	15.5	100	115.0	1.0	4.00	8.15	4.15	
	3.8	100	115.0	1.0	3.83	7.15	3.96	
	3.8	100	114.8	1.2	3.52	6.34	4.08	4.06
	3.8	100	114.6	1.4	3.21	5.69	4.13	
Pyroceram 9606	31.0	100	114.0	1.2	3.41	8.34	3.72	3.72
	15.5	100	114.0	1.0	3.62	8.02	3.73	
	15.5	100	113.8	1.2	3.14	7.03	3.62	3.69
	15.5	100	113.6	1.4	2.90	6.35	3.71	
	3.8	100	114.0	1.0	3.66	6.92	3.78	
	3.8	100	113.8	1.2	3.25	6.03	3.76	3.71
	3.8	100	113.6	1.4	2.82	5.43	3.61	

Table 4. Further examples of the reduced data.

Sample	P (MPa)	T_{rock} (°C)	T_{htr} (°C)	P.R.	$\lambda_{apparent}$ (W/m·K)	Power (W)	λ_{actual}	$\bar{\lambda}_{actual}$
TP9	31.0	28	44.0	1.0	6.27	10.72	6.25	
	31.0	28	43.8	1.2	5.46	9.55	6.07	6.13
	31.0	28	43.6	1.4	4.95	8.65	6.08	
	15.5	28	44.0	1.0	5.53	8.54	5.82	
	15.5	28	43.8	1.2	4.91	7.66	5.77	5.84
	15.5	28	43.6	1.4	4.56	7.08	5.93	
	3.8	28	44.0	1.0	5.20	7.14	5.47	
	3.8	28	43.8	1.2	4.68	6.41	5.50	5.49
	3.8	28	43.6	1.4	4.24	5.85	5.51	
	31.0	100	115.0	1.0	4.38	10.80	4.30	
	31.0	100	114.8	1.2	3.90	9.58	4.28	4.28
	31.0	100	114.6	1.4	3.50	8.57	4.25	
	15.5	100	115.0	1.0	4.30	9.26	4.47	
	15.5	100	114.8	1.2	3.80	8.17	4.42	4.43
	15.5	100	114.6	1.4	3.42	7.34	4.40	
	3.8	100	114.6	1.4	3.34	6.72	4.30	
	3.8	100	114.8	1.2	3.77	7.49	4.39	4.40
	3.8	100	115.0	1.0	4.32	8.44	4.50	
	31.0	200	213.0	1.0	3.89	9.34	3.79	
	31.0	200	212.8	1.2	3.48	8.40	3.80	3.79
	31.0	200	212.6	1.4	3.13	7.49	3.79	
	15.5	200	213.0	1.0	3.88	8.82	4.01	
	15.5	200	212.8	1.2	3.46	7.82	4.01	4.00
	15.5	200	212.6	1.4	3.11	7.01	3.99	
	3.8	200	212.6	1.4	3.03	6.71	3.89	
								3.93
	3.8	200	213.0	1.0	3.83	8.41	3.96	

Discussion

Thermal Conductivity

Thermal conductivity of the five rock salt samples decreases monotonically with increasing temperature. Any pressure effect on the data is exceedingly small. In Fig. 5, there is no obvious order to the five data points (i.e., pressures) between any of the temperatures in any of the runs, but this assertion has not been checked quantitatively. If the measurement reproducibility is taken as ± 0.25 W/m·K as estimated below, then any pressure effect on λ is easily less than ± 0.1 W/m·K over the 30-MPa range measured here.

Compared run to run in Fig. 7, the conductivities of samples TP7, TP8, TP9, and TP11 are indistinguishable over the entire (P,T) range (Fig. 5). The fifth sample, TP10, which would be expected to closely resemble TP11 on the basis of Table 1, has a distinctly higher conductivity than the others. Excepting TP10, the rock salt measured here is less conductive, by 0.5 to 1.0 W/m·K, than pure halite (Yang, 1981) but still considerably more conductive than most crystalline rocks (see, for instance, Touloukian and Ho, 1981). The temperature sensitivity of the conductivity of TP10 is strong, and TP10 actually shows a higher conductivity than pure halite at $T < 350$ K.

Most of the relationships shown in Fig. 7 are reasonable. It is likely that the nonhalite components of the rock salt samples measured here have a lower conductivity than halite. The conductivity of anhydrite is reported in the Touloukian and Ho (1981) compendium as 5.1 ± 0.6 W/m·K; values are not available for clay minerals. Therefore, the conductivity of the bulk rock should be somewhat lower than that of pure halite, depending on morphological relationships between the different phases (see, for instance, Walsh and Decker, 1966).

Acton (1978) measured the thermal conductivity of a number of rock salts with >50% halite content and found conductivities at room temperature increasing from 3 to 8 W/m·K with increasing halite concentration. Note that the conductivity of a nearly pure rock salt from Avery Island, La., is essentially identical to that of halite (Durham et al., 1981). The conductivity of TP10, therefore, is unusually high at $T < 400$ K. While a petrographic examination of the sample has not been made, the "normal" results from a sample immediately adjacent (TP11) suggest nothing abnormal about the composition of rock at this depth. However, the diffusivity of TP10 is also relatively high at the lower temperatures (Fig. 8). In most situations, conductivity and diffusivity are related according to

$$\kappa = \frac{\lambda}{\rho C_p} \quad , \tag{3}$$

where

ρ is the density, and

C_p is the specific heat at constant pressure.

Therefore, the consistency of the high conductivity and diffusivity suggests that TP10 really is physically or chemically different from the other Permian Basin salt samples.

The lack of a pressure effect in our measurements is also reasonable but would not be reasonable for almost any other crystalline rock. Confining pressure in the range up to 200 MPa, which is applicable to the upper crust, typically has a pronounced effect on many rock physical properties, such as strength, transport properties, and elastic moduli. Most of these effects can be related to the effect that pressure has on the microfractures pervading most rocks: pressure acts to hold closed existing cracks and to prevent new ones from being created. In contrast to most other rocks, rock salt is composed of a single mineral, halite, whose symmetry is cubic.

Two important causes of microfractures in other rocks, but less important in rock salt, are elastic mismatches under a change in lithostatic load and thermal expansion mismatches under uniform heating. Durham et al. (1981) also found Avery Island rock salt to have thermal properties that are independent of pressure. It should be pointed out that the pressure effects discussed here pertaining to the upper crust are extrinsic effects, to be contrasted with intrinsic effects seen at higher pressures. Above 1 GPa, the halite lattice itself becomes sufficiently compressed that increases in the thermal transport properties are readily detectable (Bridgman, 1952; Fujisawa et al., 1968; Kieffer et al., 1976; Yukutake and Shimada, 1978).

Rock salt has another atypical physical property that relates to the absence of a pressure effect in our measurements: a relatively low plastic flow strength (Carter and Heard, 1970; Carter and Hansen, 1980). Fractures that do form in rock salt through, for example, the application of a nonuni-

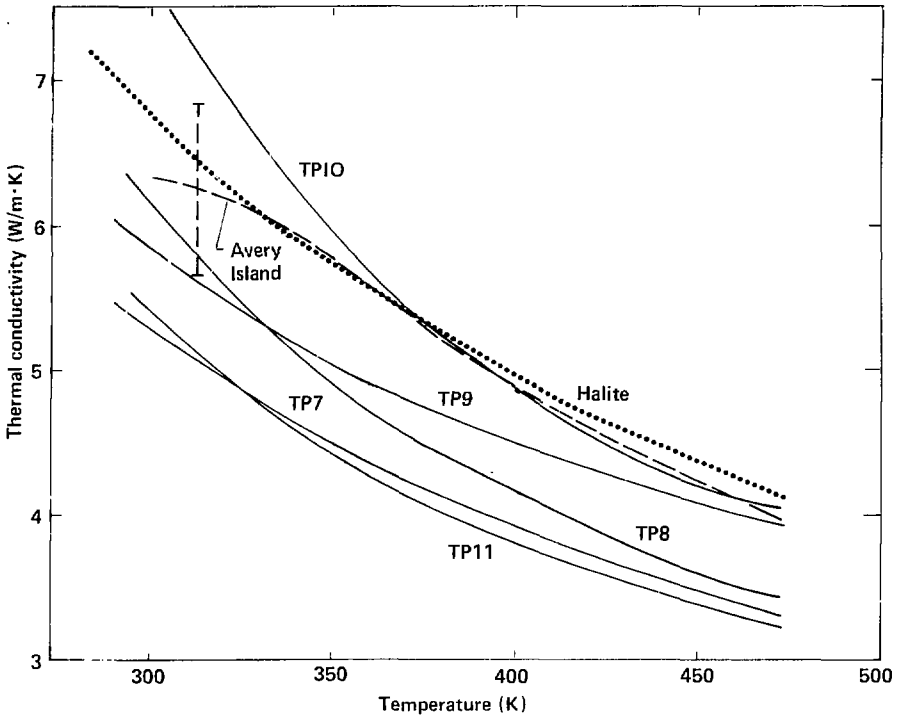

Figure 7. Summary of thermal conductivity measurements for salt. The solid lines are estimated fits to the data in Fig. 5. The error bar shows the scatter in the Avery Island data, which are taken from Durham et al. (1981).

form load or nonuniform temperature change, can be closed permanently by plastic deformation under modest pressures even at room temperature (ductility increases as temperature increases).

Sutherland and Cave (1980) and Wawersik and Hannum (1980) found that permanent reductions in room pressure porosity occurred in rock salt following pressurization to between 10 and 30 MPa. This effect is very important to laboratory testing of core samples. A coring operation applies nonuniform stresses to the core and may therefore damage it (i.e., introduce fractures and microfractures) When tested in the laboratory that core may exhibit differing physical properties at low pressures (e.g., 0.1 MPa) depending on whether it had been pressurized after coring. Note in particular that our sample preparation treatment involved an initial pressurization at 10–12 MPa and that our test matrix began at $P = 31$ MPa (Fig. 4). In the case of Avery Island salt, thermal conductivity measurements on core at 0.1 MPa are substantially lower if the core has not been pressurized (Morgan, 1979) than if it has been pressurized (Durham et al., 1981).

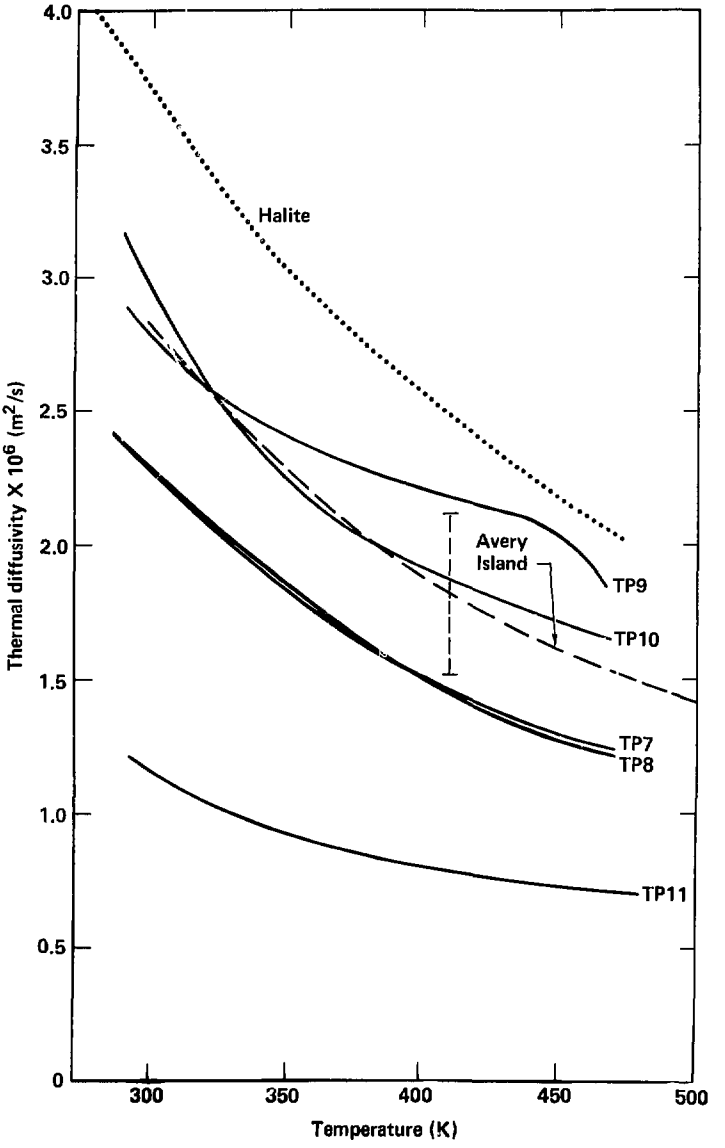

Figure 8. Summary of thermal diffusivity measurements for salt. The solid lines are estimated fits to the data in Fig. 6. The error bar shows the scatter in the Avery Island data, which are taken from Durham et al. (1981).

Thermal Diffusivity

Thermal diffusivity in Permian Basin rock salt decreases with increasing temperature, consistent with previous findings for salt (Durham et al., 1981; Yang, 1981). We cannot exclude the possibility of a pressure effect on diffusivity. At room temperature, the diffusivity of all five salt samples shows qualitatively (Fig. 6) a positive dependence on confining pressure. At 400 K, the only other temperature at which pressure was varied, the pressure dependence is ambiguous. There is no basis in the Pyroceram results in Fig. 6 to suggest that the effect is apparatus-dependent. On the other hand, to the extent that Eq. (3) applies to our experiment, any pressure effect on κ would have to result in a pressure effect on λ. (The effect of pressure on ρC_p is relatively small in low-porosity materials.)

We observe the pressure effect on κ and λ to be different, which suggests some difference in the physical mechanism of heat transport, in our experiment at least, between the transient and steady-state heat flow situations. It is plausible but by no means certain that the difference is technique-dependent, even though the Pyroceram results revealed nothing unusual: our diffusivity measurement technique requires steep thermal gradients in the sample. Salt has a high thermal expansivity (roughly an order of magnitude higher than Pyroceram and most silicate rocks) and may be prone to thermal cracking, especially at low confining pressures. We have already discussed evidence that cracks in rock salt, once formed, are closed tight or healed at modest temperatures and pressures. Thus, if the diffusivity technique did produce fractures in the rock salt, we would expect to see a positive relationship between κ and P and we would not necessarily expect to see a similar relationship between λ and P. In such a situation, the actual diffusivity of the rock salt is the value at highest confining pressure.

Figure 8 shows the relationships between diffusivity of the five samples tested here and that of Avery Island rock salt and pure halite. The relationships are very similar to those shown in Fig. 7 for conductivity. Perhaps the most unusual feature of Fig. 8 is the low diffusivity of TP11. TP11 is also the least conductive of the samples (Fig. 7) but only by a small margin. The wide difference between the diffusivity of TP11 and the other samples is not consistent with Eq. (3) and Fig. 7 and is therefore not fully believable. Again, apparatus-related effects may have been playing a role.

Measurement Resolution and Accuracy

Nearly all information related to the magnitude of the accuracy and resolution is contained in Figs. 5 and 6, where we compare our measurements on the reference standard with known values. The scatter in conductivity measurements at a given temperature on a given run seems typically to be $< \pm 0.25$ W/m·K. Two of the causes are identified as thermocouple resolution at the 0.1-K level and noise in the control of the center (inner) heater power. The latter is roughly ± 0.05 W/m·K, the typical standard deviation of a given measurement group of 15 to 20 records (e.g., Table B4 in Appendix B). A third cause is noise in the power ratio (P.R.). Over the same averaged group, P.R. shows (Table B4 again gives a typical value) a standard deviation of approximately $\pm 3\%$ around nominal which, on the basis of Fig. A1 in Appendix A, should contribute approximately ± 0.1 W/m·K to the noise in Fig. 5. The quasi-random error in the confining pressure should not be a direct noise maker, given our conclusion that λ is independent of P.

The conductivity data on Pyroceram have been worked through the correction procedure (Appendix A), which has essentially forced them to perfect accuracy. The only factors that could therefore affect the accuracy of the salt conductivity data are (a) the accuracy of the correction procedure (Appendix A) and (b) systematic changes occurring from run to run. Any inaccuracy in the correction procedure must be second order, since the salt and Pyroceram have nearly the same conductivity. The very reason for selecting a standard of conductivity near 4 W/m·K was to minimize the first category of error.

Minor errors in thermocouple position caused by drift of the drill bit during sample machining introduce a systematic error of the second category. Based on post-test examination of TP9, the precision on the value of r used in the data reduction was ± 1.0 mm at all radii (Table 2). A rough calculation based on Fig. B1 in Appendix B indicates that the worst distribution of this error among the six thermocouples (i.e., a -1-mm error in the position of the first thermocouple and a $+1$-mm error in that of the sixth thermocouple) leads to a 7% error in λ. In a real sample such as TP9 (Table 2), therefore, where the distribution of error is random, the resultant systematic error in λ can be expected to be much less than 7%. Little else is known concerning the second category of error because we did not repeat runs on the same piece of material. The proximity of conductivity

results of TP7, 8, 9, and 11 is encouraging that systematic problems are small, but the results of TP10 question such a conclusion. Future runs on the reference standard will help resolve the problem.

The scatter in diffusivity measurements on the Pyroceram reference standard (Fig. 6) is approximately $\pm 0.1 \times 10^{-6}$ m^2/s at all temperatures measured. We have not performed a sufficiently detailed parameter sensitivity study of the iterative data reduction routine to determine quantitatively the causes of scatter. Qualitatively, the most important factors are a somewhat nonreproducible heat flow pattern in the rock (estimated by Abey et al., 1982, to influence κ by less than $\pm 5\%$) and the 0.1 K round-off error in thermocouple readings. As discussed above, the apparent pressure effect on diffusivity at 300 K and the combined results for diffusivity and conductivity suggest that the apparatus may systematically deflect diffusivity measurements downwards at lower P and low T, where the rock is less ductile and more prone to cracking introduced by thermal gradients.

Conclusions

We made measurements of thermal conductivity λ and thermal diffusivity κ on five 100-mm diameter by 250-mm length rock salt cores from the Detten #1 and G. Friemel #1 wells in the Permian Basin Cycle 4 and Cycle 5 formations in Deaf Smith County, Tex. Measurement temperatures T covered $300 < T < 473$ K and pressures P covered $0.1 < P < 30$ MPa. We found the following:

1. Thermal conductivity λ does not exhibit a dependence upon P beyond the measurement resolution ± 0.25 W/m·K. Comparing groups of measurements of λ indicates that the variation of λ over the range of P used in the experiments is $< \pm 0.10$ W/m·K.

2. Thermal conductivity λ exhibits a monotonic, negative temperature dependence in all five samples tested. Values were generally lower than for pure halite at any T, perhaps reflecting the 5–20% nonhalite component of the rocks. For four of the five samples, λ fell from 5.6 ± 0.5 W/m·K at room temperature to 3.6 ± 0.3 W/m·K at 473 K, i.e., approximately 20% below the curve for pure halite. The fifth sample showed $\lambda = 7.7$ W/m·K (± 0.25 W/m·K) at room temperature, falling to 4.25 ± 0.25 W/m·K at 473 K.

3. Thermal diffusivity κ also exhibits a monotonic, negative temperature dependence. Above room temperature, κ does not vary with confining pressure beyond the measurement resolution $\pm 0.1 \times 10^{-6}$ m^2/s. A positive relationship between κ and P, which we observed mainly at room temperature, may have been an artifact of the high temperature gradients imposed during the measurement process.

4. For four of the five samples, κ fell from $2.7 \pm 0.4 \times 10^{-6}$ m^2/s at room temperature to $1.5 \pm 0.3 \times 10^{-6}$ m^2/s at 473 K. For the fifth sample, κ was inexplicably lower, decreasing from 1.2×10^{-6} m^2/s at room temperature to 0.7×10^{-6} m^2/s at 473 K.

Appendix A
The Conductivity Measurement Technique

The geometry of the sample assembly and internal heater (Fig. 3) is intended to simulate an infinite line source heat flow pattern in the volume of rock near the tips of the six sample thermocouples. Such a heat flow pattern facilitates data reduction since a simple analytical relationship applies:

$$T(r) = \frac{q}{2\pi\lambda} \log_e r \quad . \tag{A1}$$

The various symbols in Eq. (A1) are defined in the text. The desired heat flow pattern is achieved with the sectioned internal heater; the guard sections are powered at a level slightly higher than the central section to compensate for axial heat flow from the central section. Note that if Eq. (A1) is used to reduce experimental data gathered in the situation where the power ratio (P.R.) = 1 (P.R. is defined as the ratio of power per unit length of the guard vs central sections), the central heater will supply an excess of power as compared to the correct [for Eq. (A1)] situation, and the apparent conductivity $\lambda_{apparent}$ will be greater than the true conductivity λ_{actual}. As P.R. increases, $\lambda_{apparent}$ approaches λ_{actual} and eventually falls below λ_{actual}. It turns out that it is difficult to identify experimentally the exact P.R. for which $\lambda_{apparent} = \lambda_{actual}$.

We resolved the problem by simulating the system numerically and calibrating the simulation with a material of known conductivity (i.e., the Pyroceram 9606 reference standard). In doing so, we actually loosened an important experimental restriction: the numerical simulation, to the extent it is accurate, allows determination of λ_{actual} for any steady-state heat flow pattern; thus, it is not necessary to operate at the "correct" P.R. for Eq. (A1). In fact, it is not even necessary to know the correct P.R. to determine λ_{actual}, although it is easy enough to identify the correct P.R. with the simulation.

We performed the simulation with the computer program TRUMP (Edwards, 1972). The parameters for the model were the geometrical arrangement and thermal properties of all parts of the system. The conductivity of the sample, λ_{actual}, was one of these parameters. The model operated like the experiment: an ambient P (pressure) and T (temperature) were selected (so that the model would select proper conductances in the system), as were a P.R. and central heater power. The output was simply an apparent conductivity: λ_{app}^{calc}. As it turned out, λ_{app}^{calc} was very insensitive to (P,T) and absolute power level, and it depended primarily on λ_{actual} and P.R. It became possible, therefore, to reduce the modeling work to curves of λ_{actual} vs λ_{app}^{calc} for the three power ratios used in the experiments: 1.0, 1.2, and 1.4. Figure A1 illustrates insensitivity of the model to T and power level, and the curves for the three power ratios.

The curves in Fig. A1 represent the uncalibrated numerical model. The trends in experimental vs calculated values of $\lambda_{apparent}$ for Pyroceram are plotted in Fig. A2 against P,T, and P.R. Calculated values of $\lambda_{apparent}$ are consistently higher than measured values, meaning that a correction needs to be applied to λ_{app}^{exp} before the relationships in Fig. A1 can be exploited to finally determine λ_{actual}. In the strictest sense, a different correction factor is needed for each of the 90 different sets of (P.R., P, and T). However the dependencies on P.R. and T shown in Fig. A2 are sufficiently indistinct that only five different correction factors were used, one for each pressure (Table A1).

All data, then, regardless of P.R. or adherence to Eq. (A1), can be used to determine λ_{actual}. The procedure, detailed in Appendix B is

1. Find λ_{app}^{exp} by applying the raw data to Eq. (A1).
2. Find λ_{app}^{calc} by applying the appropriate correction factor from Table A1.
3. Find λ_{actual} from the curves in Fig. A1.

We cannot explain the cause of the 10–15% error in λ_{app}^{calc} vs λ_{app}^{exp} (Table A1) within the TRUMP model. In fact, as regards simulation of other aspects of the system, the model has been excellent. For instance, conductivity in the simulation, λ_{app}^{calc}, was found to be insensitive to power input; repeat tests at varying power levels at 338 K on the Pyroceram confirmed (within considerable noise) that the real world behaved the same way (Fig. A3). Another confirmation of the model is the fact that λ_{actual} was found to be independent of P.R. (Table 3); obviously the true conductivity of the standard has nothing to do with P.R. (it depends only on T as shown in Fig. 2).

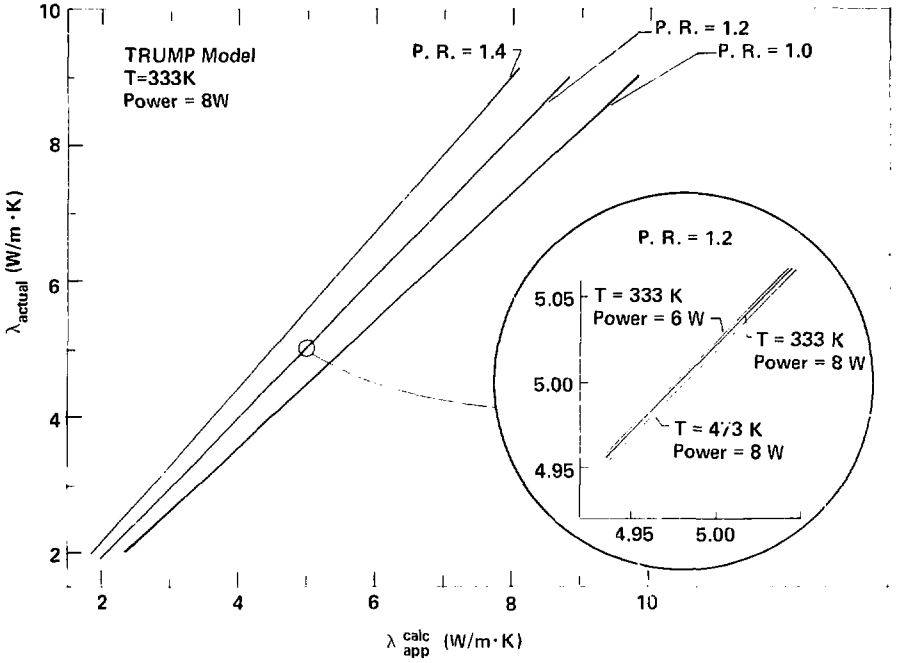

Figure A1. The numerical simulation of the experiment using the TRUMP routine. The inset shows the insensitivity of the model to inner heater power and to ambient temperature.

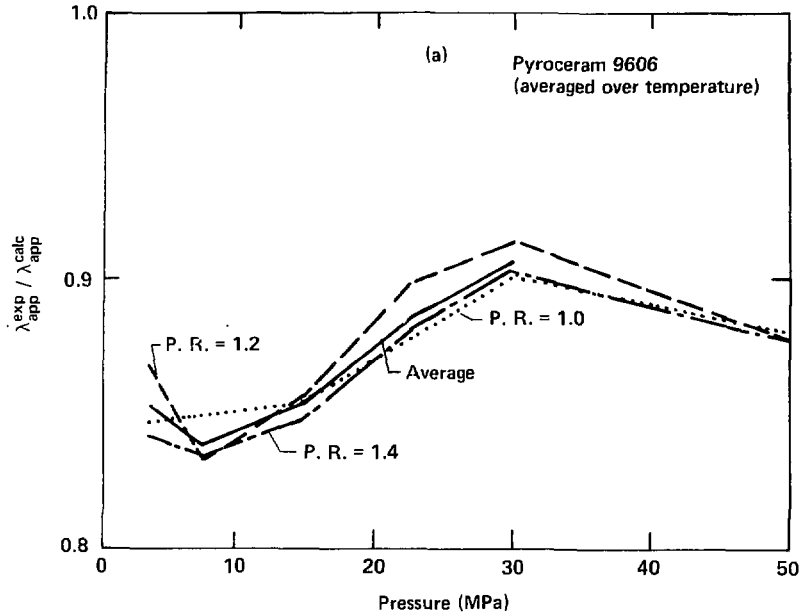

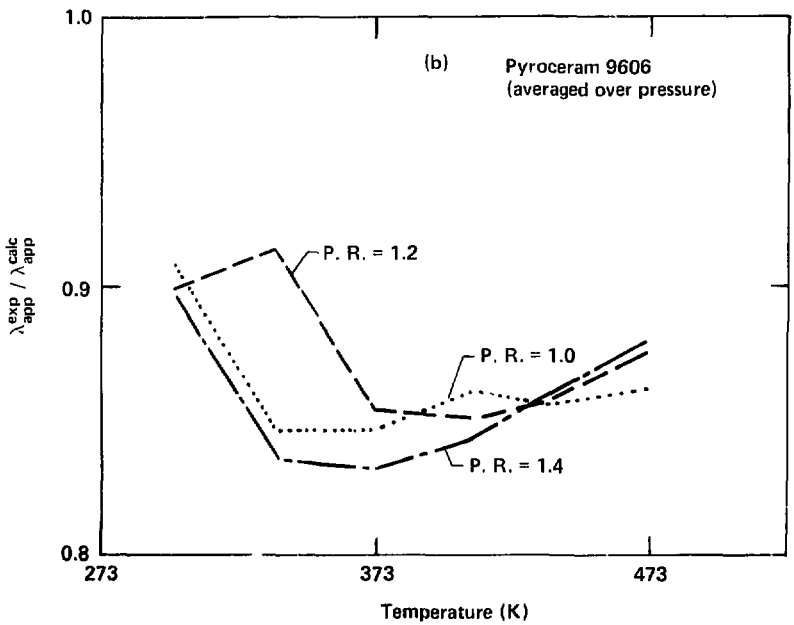

Figure A2. Comparison of the TRUMP model to the actual experiment at three different power ratios P.R. The data plot labelled "Average" shows the corrections used in the application of the model.

Table A1. Correction factors from Fig. A2.

Pressure (MPa)	$\lambda_{app}^{exp} / \lambda_{app}^{calc}$
31.0	0.905
23.3	0.886
15.5	0.853
7.8	0.838
3.8	0.852

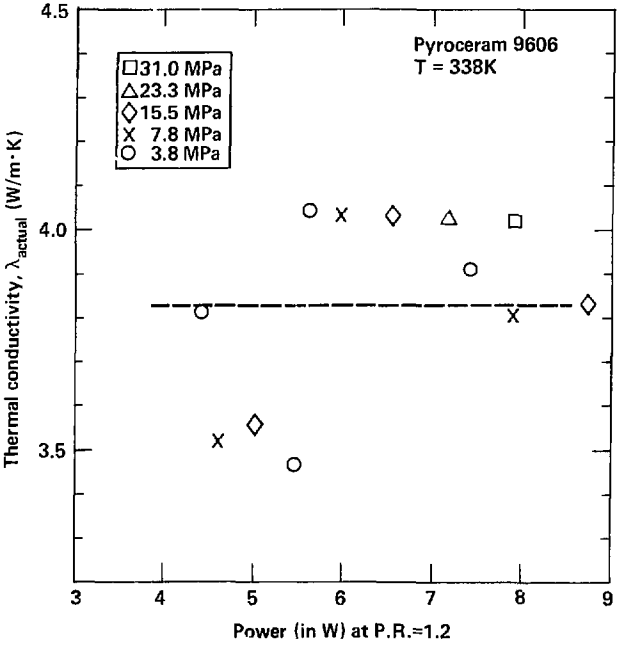

Figure A3. Illustration of the independence of measured conductivity and inner heater power. The dashed line shows the true conductivity of Pyroceram 9606 at T = 338 K.

Appendix B
Data Reduction Example of Conductivity

As an example, we show in Appendix B the data treatment from start to finish of a point at the approximate center of gravity of the tests for sample TP9, P (pressure) = 15.5 MPa, T (temperature) = 373 K, and P.R. (power ratio) = 1.2.

Tables B1 and B2 list raw data and Tables B3 and B4 show intermediate steps in the data reduction. Figure B1 illustrates a detail of the reduction process. The final step in the data reduction, find λ_{actual} (the *true conductivity*) from the curves in Fig. A1, is illustrated by the examples in Tables 3 and 4. In detail the process is as follows.

First, we gathered the raw data in Table B1 to zero the six sample thermocouples, whose absolute accuracy (approximately ±1 K) is far worse than what is ultimately required. While these data were gathered, the internal heaters were off. We made repeat readings at approximately 7 min intervals. We then examined Table B1 data to find the point where temperatures had stabilized. Records at the top showing nonstabilized temperatures, and two or three subsequent records were eliminated. In the present example, we ignored the top 11 records in Table B1, then we averaged the readings of the six sample thermocouples (Table B3).

As the data in Table B2 were gathered (again, one record every 7 min), the internal heaters were turned on, with the set points for P.R. and temperature of the central section of the heater held constant. Table B2 data were reduced using the average "zero temperatures" of Table B3, as shown in Table B4. As with Table B3, only steady-state data were used in Table B4. Steady state existed from the start in this example (not an unusual situation), so only the first two records in Table B2 were eliminated in Table B4. For a given record, the six sample thermocouples were first normalized by their "zero" readings (Table B3), then fit to a straight line on T vs $\log_e r$ axes. According to Eq. (2), such a line has a slope of $q/2\pi\lambda$, where λ is more appropriately called $\lambda_{apparent}$. Figure B1 illustrates the fit for the first record in Table B4. The quantity q is simply the power of the central section (also listed in Table B4) divided by the length of the central section, 76.2 mm. For any given set of (P, T, P.R.), 15 to 20 records were made; therefore, the length of Table B4 is typical. We manipulated each record thusly and calculated the average values of $\lambda_{apparent}$, power, P, P.R., and sample Ts. We then listed the values of $\lambda_{apparent}$, power, and P.R. in the master data tables (of which Tables 3 and 4 are extracts) and applied the remaining two steps outlined in Appendix A to determine λ_{actual}.

Table B1. Example of raw data under ambient conditions. (See Table B2 for explanation.)

4.000	22.000	2.000	12.000	0.000	0.000	0.000	0.000	0.000	0.000
0.002	0.230	94.700	94.000	95.100	94.800	95.700	95.400	96.100	95.700
96.400	94.300	21.700	21.000	95.300	94.500	96.500	95.700	97.300	90.[illegible]00
96.100	96.800	96.400	97.800	22.700	95.500	95.500	96.100	22.900	67.800
4.000	22.000	7.000	13.000	0.000	0.000	0.001	0.000	0.000	0.000
0.001	0.187	94.100	93.400	94.500	94.900	95.900	95.400	96.200	95.[illegible]00
96.500	95.100	21.800	21.000	94.700	93.900	96.000	95.100	96.400	94.800
96.000	96.700	96.300	98.500	22.700	95.900	96.300	96.000	22.900	71.300
4.000	22.000	14.000	28.000	0.000	0.000	0.000	0.000	0.001	0.[illegible]00
0.001	0.187	94.100	93.500	94.600	94.900	95.900	95.400	96.200	95.600
96.500	95.200	21.700	21.000	95.100	94.500	96.100	95.100	96.500	95.[illegible]00
96.000	96.700	96.300	98.400	22.700	95.900	96.300	96.000	22.900	73.[illegible]00
4.000	22.000	21.000	44.000	0.000	0.000	0.000	0.000	0.001	0.000
0.002	0.186	94.200	93.500	94.700	94.900	95.900	95.400	96.200	95.[illegible]00
96.500	95.200	21.800	21.000	95.200	94.600	96.100	95.100	96.400	95.200
96.100	96.700	96.300	98.400	22.700	95.900	96.400	96.100	22.900	73.700
4.000	22.000	29.000	0.000	0.000	0.000	0.000	0.000	0.001	0.[illegible]00
0.002	0.186	94.300	93.600	94.700	94.900	96.000	95.400	96.200	95.700
96.500	95.200	21.700	21.000	95.300	94.700	96.100	95.100	96.400	95.300
96.000	96.700	96.300	98.000	22.700	95.900	95.900	96.000	22.900	73.[illegible]00
4.000	22.000	36.000	15.000	0.000	0.000	0.000	0.000	0.001	0.000

Table B1. Continued.

0.000	0.185	94.300	93.600	94.800	95.000	96.000	95.500	96.300	95.700
96.500	95.200	21.700	20.900	95.300	94.700	96.100	95.200	96.500	95.[illegible]00
96.000	96.800	96.300	97.600	22.700	96.000	95.400	96.100	22.900	74.000
4.000	22.000	43.000	31.000	0.000	0.000	0.000	0.000	0.000	0.[illegible]00
0.001	0.184	94.300	93.600	94.800	95.000	96.100	95.500	96.300	95.700
96.600	95.200	21.700	20.900	95.400	94.700	96.100	95.200	96.500	95.300
96.100	96.700	96.300	97.800	22.700	96.000	95.600	96.000	22.900	74.[illegible]00
4.000	22.000	50.000	46.000	0.000	0.000	0.001	0.000	0.001	0.000
0.001	0.183	94.300	93.600	94.800	95.000	96.100	95.500	96.300	95.700
96.600	95.200	21.800	21.000	95.400	94.800	96.100	95.200	96.400	95.[illegible]00
96.000	96.700	96.300	98.200	22.700	95.900	96.000	96.100	22.900	74.100
4.000	22.000	58.000	2.000	0.000	0.000	0.001	0.000	0.000	0.000
0.002	0.182	94.400	93.600	94.900	95.000	96.100	95.500	96.300	95.[illegible]00
96.600	95.200	21.700	21.000	95.400	94.800	96.100	95.200	96.500	95.300
96.000	96.700	96.300	98.500	22.700	96.000	96.400	96.000	22.900	74.200
4.000	23.000	5.000	18.000	0.000	0.000	0.001	0.000	0.001	0.000
0.001	0.182	94.400	93.700	94.900	95.000	96.100	95.500	96.300	95.800
96.600	95.200	21.800	21.000	95.500	94.800	96.100	95.200	96.500	95.[illegible]00
96.000	96.800	96.300	98.600	22.700	96.000	96.500	96.000	22.900	74.200
4.000	23.000	12.000	33.000	0.000	0.000	0.001	0.000	0.000	0.000
0.001	0.181	94.400	93.700	94.900	95.000	96.100	95.500	96.300	95.[illegible]00
96.600	95.200	21.700	21.000	95.500	94.800	96.100	95.200	96.500	95.300
96.100	96.800	96.300	98.300	22.700	96.000	96.300	96.100	22.900	74.200
4.000	23.000	19.000	48.000	0.000	0.000	0.001	0.000	0.000	0.[illegible]00
0.002	0.180	94.400	93.700	94.900	95.100	96.100	95.500	96.300	95.800
96.600	95.200	21.800	21.000	95.400	94.800	96.100	95.200	96.500	95.300
96.100	96.700	96.300	98.200	22.700	96.000	96.200	96.100	22.900	74.[illegible]00
4.000	23.000	27.000	4.000	0.000	0.000	0.001	0.000	0.000	0.000
0.003	0.179	94.400	93.700	94.900	95.100	96.100	95.600	96.400	95.[illegible]00
96.600	95.200	21.700	20.900	95.500	94.800	96.100	95.200	96.500	95.300
96.000	96.700	96.300	97.900	22.700	96.000	95.900	96.000	22.900	74.300
4.000	23.000	34.000	20.000	0.000	0.000	0.001	0.000	0.001	0.[illegible]00
0.001	0.179	94.400	93.700	94.900	95.100	96.100	95.600	96.300	95.800
96.600	95.200	21.700	21.000	95.500	94.800	96.200	95.200	96.400	95.300
96.000	96.800	96.300	97.800	22.700	96.000	95.600	96.100	22.900	74.[illegible]00
4.000	23.000	41.000	35.000	0.000	0.000	0.000	0.000	0.001	0.000
0.001	0.178	94.400	93.700	94.900	95.100	96.100	95.600	96.400	95.800
96.600	95.200	21.700	21.000	95.500	94.800	96.200	95.200	96.500	95.[illegible]00
96.000	96.700	96.300	97.600	22.700	96.000	95.400	96.000	22.900	74.300
4.000	23.000	48.000	51.000	0.000	0.000	0.001	0.000	0.001	0.[illegible]00
0.002	0.177	94.400	93.700	94.900	95.100	96.100	95.500	96.400	95.800
96.600	95.200	21.800	21.000	95.500	94.800	96.100	95.200	96.500	95.700
96.100	96.700	96.300	97.900	22.700	96.000	95.700	96.000	22.900	74.[illegible]00
4.000	23.000	56.000	6.000	0.000	0.000	0.001	0.000	0.001	0.000
0.001	0.176	94.400	93.700	94.900	95.100	96.100	95.600	96.400	95.800
96.600	95.200	21.700	20.900	95.500	94.800	96.100	95.200	96.500	95.[illegible]00
96.000	96.700	96.300	98.500	22.700	96.000	96.300	96.000	22.900	74.300
5.000	0.000	3.000	22.000	0.000	0.000	0.002	0.000	0.000	0.000
0.002	0.176	94.400	93.700	94.900	95.100	96.100	95.600	96.400	95.[illegible]00
96.700	95.200	21.700	21.000	95.400	94.800	96.200	95.200	96.500	95.300
96.300	96.700	96.300	98.700	22.700	96.000	96.600	96.000	22.900	74.300
5.000	0.000	10.000	38.000	0.000	0.000	0.001	0.000	0.001	0.000
0.002	0.175	94.400	93.700	94.900	95.100	96.100	95.500	96.400	95.800
96.600	95.200	21.700	20.900	95.500	94.800	96.200	95.200	96.500	95.[illegible]00
96.000	96.800	96.300	98.500	22.600	96.000	96.500	96.100	22.800	74.300
5.000	0.000	17.000	53.000	0.000	0.000	0.000	0.000	0.000	0.000
0.002	0.174	94.400	93.700	94.900	95.100	96.100	95.500	96.400	95.[illegible]00

Table B1. Continued.

96.600	95.200	21.700	20.900	95.500	94.800	96.200	95.200	96.500	95.300
96.000	96.800	96.300	98.200	22.700	96.000	96.200	96.000	22.800	74.300
5.000	0.000	25.000	9.000	0.000	0.000	0.001	0.000	0.000	0.000
0.002	0.173	94.400	93.700	94.900	95.100	96.100	95.500	96.400	95.800
96.600	95.200	21.700	20.900	95.500	94.800	96.100	95.200	96.500	95.300
96.000	96.700	96.300	97.800	22.700	96.000	95.700	96.100	22.800	74.300
5.000	0.000	32.000	24.000	0.000	0.000	0.001	0.000	0.000	0.000
0.001	0.173	94.400	93.700	94.900	95.100	96.200	95.600	96.400	95.800
96.700	95.300	21.600	20.900	95.500	94.800	96.200	95.200	96.500	95.300
96.000	96.700	96.400	97.600	22.600	96.000	95.400	96.100	22.800	74.300
5.000	0.000	39.000	40.000	0.000	0.000	0.000	0.000	0.000	0.000
0.001	0.172	94.400	93.700	94.900	95.100	96.200	95.600	96.400	95.800
96.700	95.300	21.400	20.700	95.500	94.800	96.200	95.200	96.600	95.400
96.000	96.700	96.300	97.900	22.400	96.000	95.600	96.000	22.600	74.200
5.000	0.000	46.000	55.000	0.000	0.000	0.001	0.000	0.000	0.000
0.002	0.171	94.400	93.700	94.900	95.100	96.100	95.600	96.400	95.800
96.700	95.300	21.400	20.700	95.500	94.800	96.200	95.200	96.500	95.300
96.000	96.700	96.400	98.100	22.400	96.000	95.900	96.000	22.600	74.200
5.000	0.000	54.000	11.000	0.000	0.000	0.001	0.000	0.000	0.000
0.002	0.170	94.400	93.700	94.900	95.100	96.100	95.600	96.400	95.800
96.600	95.300	21.600	20.800	95.500	94.800	96.100	95.300	96.500	95.400
96.000	96.700	96.300	98.700	22.500	96.000	96.500	96.000	22.700	74.200
5.000	0.000	59.000	13.000	0.000	0.000	0.000	0.000	0.000	0.000
0.001	0.184	94.400	93.700	94.900	95.100	96.100	95.600	96.400	95.800
96.600	95.300	21.600	20.800	95.300	95.000	96.200	95.300	96.500	95.300
96.000	96.700	96.400	98.100	22.500	96.100	96.100	96.000	22.700	75.500
0.000	0.000	0.000	0.000	0.000	0.000	0.000	0.000	0.000	0.000
0.000	0.000	0.000	0.000	0.000	0.000	0.000	0.000	0.000	0.000
0.000	0.000	0.000	0.000	0.000	0.000	0.000	0.000	0.000	0.000
0.000	0.000	0.000	0.000	0.000	0.000	0.000	0.000	0.000	0.000

Table B2. Example of raw data for conductivity measurements.

4.000	2.000	3.000	24.000	0.000	0.624	7.613	0.619	7.631	0.557
6.987	0.174	116.600	114.900	116.600	102.700	102.400	101.400	101.400	100.500
99.300	95.700	21.400	20.900	98.200	97.200	96.300	95.700	96.500	95.200
96.100	96.800	96.600	98.700	22.600	96.300	96.300	96.100	22.800	74.700
4.000	2.000	10.000	40.000	0.000	0.632	7.700	0.627	7.726	0.564
7.070	0.173	116.500	114.800	116.500	102.700	102.400	101.300	101.400	100.500
99.300	95.700	21.500	20.900	98.300	97.200	96.300	95.700	96.500	95.200
96.100	96.900	96.600	98.900	22.600	96.300	96.600	96.100	22.800	74.700
4.000	2.000	17.000	57.000	0.000	0.630	7.682	0.627	7.726	0.564
7.070	0.172	116.500	114.800	116.500	102.700	102.400	101.300	101.400	100.400
99.300	95.700	21.500	20.900	98.300	97.200	96.400	95.700	96.600	95.200
96.000	96.800	96.600	98.800	22.600	96.300	96.600	96.000	22.800	74.700
4.000	2.000	25.000	14.000	0.000	0.630	7.670	0.627	7.726	0.564
7.069	0.172	116.500	114.800	116.500	102.700	102.400	101.400	101.400	100.500
99.300	95.700	21.500	20.900	98.200	97.200	96.300	95.700	96.500	95.300
96.000	96.800	96.600	98.400	22.600	96.300	96.200	96.100	22.800	74.700
4.000	2.000	32.000	30.000	0.000	0.631	7.681	0.627	7.727	0.564
7.070	0.171	116.600	114.800	116.500	102.700	102.400	101.400	101.400	100.500
99.300	95.700	21.500	20.900	98.300	97.200	96.300	95.700	96.500	95.200
96.000	96.800	96.600	98.000	22.600	96.300	95.700	96.000	22.800	74.700
4.000	2.000	39.000	47.000	0.000	0.607	7.411	0.621	7.656	0.557
6.993	0.170	116.400	114.700	116.400	102.700	102.400	101.400	101.400	100.500

Table B2. Continued.

99.300	95.700	21.400	20.900	98.200	97.200	96.300	95.700	96.500	95.[illegible]00
96.100	96.800	96.600	97.800	22.600	96.300	95.400	96.000	22.800	74.700
4.000	2.000	46.000	0.000	0.000	0.663	8.259	0.633	7.814	0.[illegible]69
7.139	0.181	116.400	114.800	116.500	102.700	102.500	101.400	101.400	100.500
99.300	95.700	21.400	20.900	98.100	97.300	96.[illegible]00	95.700	96.500	95.700
96.000	96.800	96.600	99.700	22.600	96.300	97.300	96.100	22.700	75.[illegible]00
4.000	2.000	53.000	17.000	0.000	0.638	7.763	0.628	7.745	0.565
7.093	0.181	116.600	114.800	116.500	102.700	102.500	101.400	101.500	100.500
99.300	95.700	21.500	20.900	98.300	97.300	96.400	95.700	96.600	95.[illegible]00
96.10[illegible]	96.900	96.600	98.700	22.600	96.300	96.500	96.100	22.800	74.800
4.0[illegible]	3.000	0.000	33.000	0.000	0.627	7.644	0.630	7.767	0.566
7.094	0.179	116.500	114.800	116.500	102.700	102.500	101.400	101.400	100.[illegible]00
99.300	95.700	21.400	20.900	98.200	97.200	96.400	95.700	96.600	95.300
96.100	96.900	96.600	97.800	22.600	96.300	95.300	96.100	22.700	74.800
4.000	3.000	7.000	50.000	0.000	0.641	7.816	0.634	7.815	0.570
7.146	0.179	116.400	114.700	116.400	102.700	102.400	101.400	101.400	100.500
99.300	95.700	21.500	20.900	98.300	97.200	96.400	95.700	96.600	95.[illegible]00
96.100	96.800	96.600	98.300	22.600	96.300	95.700	96.100	22.700	74.800
4.000	3.000	15.000	7.000	0.000	0.576	7.078	0.626	7.698	0.542
7.043	0.178	116.600	114.900	116.600	102.700	102.500	101.400	101.[illegible]00	100.500
99.300	95.700	21.400	20.900	98.300	97.200	96.400	95.700	96.600	95.300
96.100	96.800	96.600	98.600	22.500	96.300	96.200	96.100	22.800	74.700
4.000	3.000	22.000	23.000	0.000	0.615	7.488	0.635	7.813	0.[illegible]70
7.150	0.177	116.500	114.800	116.500	102.700	102.500	101.400	101.400	100.500
99.300	95.700	21.400	20.900	98.200	97.200	96.300	95.700	96.600	95.300
96.100	96.800	96.600	99.000	22.600	96.300	96.600	96.000	22.700	74.[illegible]00
4.000	3.000	29.000	40.000	0.000	0.635	7.749	0.626	7.721	0.563
7.063	0.176	116.500	114.800	116.400	102.700	102.500	101.400	101.400	100.[illegible]00
99.300	95.700	21.500	20.900	98.300	97.200	96.400	95.700	96.600	95.300
96.000	96.800	96.600	98.700	22.600	96.300	96.400	96.100	22.800	74.700
4.000	3.000	36.000	57.000	0.000	0.618	7.547	0.623	7.675	0.[illegible]09
7.011	0.175	116.600	114.900	116.500	102.700	102.500	101.400	101.400	100.500
99.300	95.700	21.400	20.900	98.300	97.200	96.400	95.700	96.600	95.700
96.100	96.800	96.600	98.600	22.600	96.300	96.300	96.100	22.800	74.[illegible]00
4.000	3.000	44.000	13.000	0.000	0.629	7.664	0.628	7.744	0.563
7.065	0.175	116.500	114.800	116.500	102.700	102.500	101.400	101.400	100.[illegible]00
99.300	95.700	21.500	20.900	98.300	97.300	96.400	95.700	96.600	95.[illegible]00
96.100	96.800	96.600	98.300	22.600	96.300	96.100	96.100	22.800	74.700
4.000	3.000	51.000	29.000	0.000	0.630	7.691	0.630	7.767	0.[illegible]65
7.092	0.174	116.500	114.800	116.500	102.700	102.400	101.400	101.400	100.500
99.300	95.700	21.400	20.800	98.300	97.200	96.400	95.700	96.600	95.300
96.100	96.900	96.600	98.000	22.500	96.300	95.700	96.000	22.700	74.[illegible]00
4.000	3.000	58.000	46.000	0.000	0.636	7.745	0.628	7.743	0.565
7.092	0.173	116.600	114.800	116.500	102.700	102.400	101.400	101.400	100.500
99.300	95.700	21.400	20.900	98.300	97.200	96.300	95.700	96.600	95.[illegible]00
96.000	96.800	96.600	97.800	22.600	96.300	95.400	96.000	22.800	74.700
0.000	0.000	0.000	0.000	0.000	0.000	0.000	0.000	0.000	0.000
0.000	0.000	0.000	0.000	0.000	0.000	0.000	0.000	0.000	0.000
0.000	0.000	0.000	0.000	0.000	0.000	0.000	0.000	0.000	0.000
0.000	0.000	0.000	0.000	0.000	0.000	0.000	0.000	0.000	0.000

Explanation of Tables B1 and B2

Tables B1 and B2 give raw data, grouped in blocks of 3 records each, 40 items (floating point numbers) per record (4 lines per record, 10 items per line).

Explanation of items in a given record (using record 3, Table B2 as an example)

Item	Explanation	Value
1–4	Day (of month), hour, minute, second	0217:57 hr, 4 March 1983*
5	Dummy item	
6	0.0989 × voltage (in V), first guard heater	6.370V
7	5 × current (in A), first guard heater	1.536A × 6.370V (= 9.787W)
8–9	Same as 6,7; second guard heater	6.340V × 1.545A (= 9.796W)
10	0.0978 × voltage, central heater	5.767V
11	5 × current, central heater	1.414A × 5.767V (= 8.154W*)
	$\left(\text{Note: power ratio} = \frac{9.787 + 9.796}{2 \times 8.154} = 1.201^*\right)$	
12	(Confining pressure − 500) × 10^{-4} (in psi)	2225 psi* = 15.34 MPa
13	Temperature, first guard heater	116.5°C
14	Temperature, central heater	114.8°C
15	Temperature, second guard heater	116.5°C
16–21	Temperature of the six sample thermocouples, ordered outwards from the center	*
22–40	Various temperatures throughout system	

* These values can be found in Table B4.

Table B3. Reduction of data in Table B1.

23:19	95.10	96.10	95.50	96.30	95.80	96.60
23:27	95.10	96.10	95.60	96.40	95.80	96.60
23:34	95.10	96.10	95.60	96.30	95.80	96.60
23:41	95.10	96.10	95.60	96.40	95.80	96.60
23:48	95.10	96.10	95.50	96.40	95.80	96.60
23:56	95.10	96.10	95.60	96.40	95.80	96.60
0: 3	95.10	96.10	95.60	96.40	95.80	96.70
0:10	95.10	96.10	95.50	96.40	95.80	96.60
0:17	95.10	96.10	95.50	96.40	95.80	96.60
0:25	95.10	96.10	95.50	96.40	95.80	96.60
0:32	95.10	96.20	95.60	96.40	95.80	96.70
0:39	95.10	96.20	95.60	96.40	95.80	96.70
0:46	95.10	96.10	95.60	96.40	95.80	96.70
0:54	95.10	96.10	95.60	96.40	95.80	96.60
0:59	95.10	96.10	95.60	96.40	95.80	96.60
N=15	95.10	96.11	95.57	96.39	95.80	96.63
	(0.00)	(0.03)	(0.04)	(0.04)	(0.03)	(0.04)

Explanation of Table B3

Each row gives the time (hour:minute), and temperature readings of the six sample thermocouples, ordered outwards from the center.

The final two rows give the number (N) of readings and the averages and standard deviations (in parentheses) of the six columns of temperatures.

Table B4. Reduction of data in Table B2.

```
                                TP0304.CND [ 6]

TZ2304:    95.1  96.1  95.6  96.4  95.8  96.6
TIME  4: 2:17:57  PRESSURE = 2225 PSI  POWER =  8.15 WATTS  P.R. = 1.201
SAMPLE TS 102.7 102.4 101.3 101.4 100.4  99.3
CONDUCTIVITY =   3.81 W/MK  (RSQ = 0.95)


TIME  4: 2:25:14  PRESSURE = 2218 PSI  POWER =  8.15 WATTS  P.R. = 1.200
SAMPLE TS 102.7 102.4 101.4 101.4 100.5  99.3
CONDUCTIVITY =   3.79 W/MK  (RSQ = 0.94)


TIME  4: 2:32:30  PRESSURE = 2211 PSI  POWER =  8.15 WATTS  P.R. = 1.202
SAMPLE TS 102.7 102.4 101.4 101.4 100.5  99.3
CONDUCTIVITY =   3.79 W/MK  (RSQ = 0.94)


TIME  4: 2:39:47  PRESSURE = 2202 PSI  POWER =  7.97 WATTS  P.R. = 1.174
SAMPLE TS 102.7 102.4 101.4 101.4 100.5  99.3
CONDUCTIVITY =   3.71 W/MK  (RSQ = 0.94)


TIME  4: 2:46: 0  PRESSURE = 2313 PSI  POWER =  8.31 WATTS  P.R. = 1.268
SAMPLE TS 102.7 102.5 101.4 101.4 100.5  99.3
CONDUCTIVITY =   3.85 W/MK  (RSQ = 0.94)


TIME  4: 2:53:17  PRESSURE = 2305 PSI  POWER =  8.20 WATTS  P.R. = 1.210
SAMPLE TS 102.7 102.5 101.4 101.5 100.5  99.3
CONDUCTIVITY =   3.81 W/MK  (RSQ = 0.94)


TIME  4: 3: 0:33  PRESSURE = 2295 PSI  POWER =  8.21 WATTS  P.R. = 1.193
SAMPLE TS 102.7 102.5 101.4 101.4 100.5  99.3
CONDUCTIVITY =   3.80 W/MK  (RSQ = 0.94)


TIME  4: 3: 7:50  PRESSURE = 2288 PSI  POWER =  8.33 WATTS  P.R. = 1.210
SAMPLE TS 102.7 102.4 101.4 101.4 100.5  99.3
CONDUCTIVITY =   3.87 W/MK  (RSQ = 0.94)


TIME  4: 3:15:  7  PRESSURE = 2279 PSI  POWER =  8.09 WATTS  P.R. = 1.111
SAMPLE TS 102.7 102.5 101.4 101.4 100.5  99.3
CONDUCTIVITY =   3.75 W/MK  (RSQ = 0.94)


TIME  4: 3:22:23  PRESSURE = 2270 PSI  POWER =  8.34 WATTS  P.R. = 1.159
SAMPLE TS 102.7 102.5 101.4 101.4 100.5  99.3
CONDUCTIVITY =   3.87 W/MK  (RSQ = 0.94)


TIME  4: 3:29:40  PRESSURE = 2262 PSI  POWER =  8.13 WATTS  P.R. = 1.213
SAMPLE TS 102.7 102.5 101.4 101.4 100.5  99.3
CONDUCTIVITY =   3.77 W/MK  (RSQ = 0.94)
```

Table B4. Continued.

```
TIME  4: 3:36:57  PRESSURE = 2254 PSI  POWER =  8.01 WATTS  P.R. = 1.191
SAMPLE TS 102.7 102.5 101.4 101.4 100.5  99.3
CONDUCTIVITY =   3.71 W/MK  (RSQ = 0.94)


TIME  4: 3:44:13  PRESSURE = 2247 PSI  POWER =  8.14 WATTS  P.R. = 1.203
SAMPLE TS 102.7 102.5 101.4 101.4 100.5  99.3
CONDUCTIVITY =   3.77 W/MK  (RSQ = 0.94)


TIME  4: 3:51:29  PRESSURE = 2237 PSI  POWER =  8.20 WATTS  P.R. = 1.201
SAMPLE TS 102.7 102.4 101.4 101.4 100.5  99.3
CONDUCTIVITY =   3.82 W/MK  (RSQ = 0.94)


TIME  4: 3:58:46  PRESSURE = 2229 PSI  POWER =  8.20 WATTS  P.R. = 1.207
SAMPLE TS 102.7 102.4 101.4 101.4 100.5  99.3
CONDUCTIVITY =   3.82 W/MK  (RSQ = 0.94)


AVERAGES FOR 15 READINGS:
POWER =  8.17(0.10)  P.R. = 1.196(0.033)  PRESS = 2256( 35)
SAMPLE TS 102.7 102.5 101.4 101.4 100.5  99.3

CONDUCTIVITY =   3.80 W/MK  (S.D. = 0.05; 15 POINTS)
          1.68 HOURS ELAPSED TIME,   4: 2:17 TO  4: 3:58
```

Explanation of Table B4

1. Line 1 gives the isothermal values of the six sample thermocouples, ordered outward from the center.

2. Each data record (e.g., Table B2) leads to three lines in Table B4:

   Line 1: *time (day of month: hour: minute: second); confining pressure; central heater power; power ratio.*

   Line 2: six sample thermocouple temperatures in °C, ordered outward from the center.

   Line 3: conductivity best fit to Eq. (2); r^2, where r is the linear-correlation coefficient (Bevington, 1969).

3. The last four lines give statistical summaries of the preceding numbers. The numbers in parentheses indicate one standard deviation.

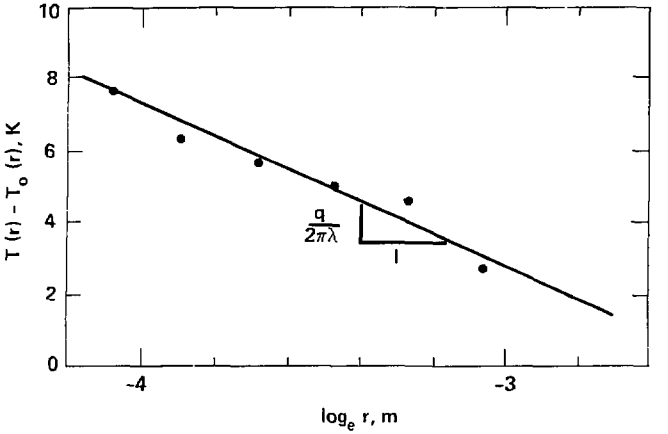

Figure B1. The best fit of the first data record in Table B4 to Eq. (B1).

Appendix C
Data Reduction Example of Diffusivity

Raw information on $T(r,t)$ is fed directly into the iterative routine that fits those data to a best value of diffusivity (κ) according to Eq. (1). Appendix C, therefore, is simply a presentation of examples of raw data.

The examples are again taken from near the center of gravity of the tests: sample TP9, P = 15.5 MPa. Table C1 shows data at room temperature and Table C2 shows data at T = 473 K. The diffusivity is higher at the lower temperature (2.72×10^{-6} m^2/s vs 1.59×10^{-6} m^2/s). It is not difficult to perceive directly from the data that the heat pulse moved more rapidly in Table C1 than in Table C2.

Table C1. Example 1 of raw data for diffusivity measurement. (See Table C2 for explanation.)

28.000	13.000	2.000	43.000	0.000	0.012	0.173	0.019	0.256	0.005
28.000	13.000	2.000	51.000	21.300	22.000	21.500	22.100	21.700	22.100
28.000	13.000	2.000	59.000	21.400	22.000	21.600	22.100	21.700	22.100
28.000	13.000	3.000	7.000	21.300	22.000	21.500	22.100	21.600	22.100
28.000	13.000	3.000	15.000	21.400	22.000	21.600	22.200	21.600	22.100
28.000	13.000	3.000	23.000	21.500	22.000	21.600	22.200	21.500	22.100
28.000	13.000	3.000	32.000	22.000	22.200	21.600	22.200	21.500	22.100
28.000	13.000	3.000	40.000	23.000	22.600	21.800	22.200	21.500	22.100
28.000	13.000	3.000	48.000	24.500	23.200	22.200	22.300	21.600	22.100
28.000	13.000	3.000	56.000	26.400	24.100	22.700	22.600	21.700	22.100
28.000	13.000	4.000	4.000	28.500	25.200	23.500	22.900	21.800	22.200
28.000	13.000	4.000	12.000	30.700	26.400	24.300	23.300	22.000	22.200
28.000	13.000	4.000	20.000	33.000	27.800	25.300	23.900	22.200	22.300
28.000	13.000	4.000	28.000	35.200	29.100	26.300	24.500	22.600	22.500
0.000	0.000	0.000	0.000	0.000	0.000	0.000	0.000	0.000	0.000
0.000	0.000	0.000	0.000	0.000	0.000	0.000	0.000	0.000	0.000
0.000	0.000	0.000	0.000	0.000	0.000	0.000	0.000	0.000	0.000
0.000	0.000	0.000	0.000	0.000	0.000	0.000	0.000	0.000	0.000
0.000	0.000	0.000	0.000	0.000	0.000	0.000	0.000	0.000	0.000
0.000	0.000	0.000	0.000	0.000	0.000	0.000	0.000	0.000	0.000
0.000	0.000	0.000	0.000	0.000	0.000	0.000	0.000	0.000	0.000
0.000	0.000	0.000	0.000	0.000	0.000	0.000	0.000	0.000	0.000
0.000	0.000	0.000	0.000	0.000	0.000	0.000	0.000	0.000	0.000
0.000	0.000	0.000	0.000	0.000	0.000	0.000	0.000	0.000	0.000

Table C2. Example 2 of raw data for diffusivity measurement.

11.000	15.000	54.000	16.000	0.001	0.015	0.172	0.021	0.226	0.007
11.000	15.000	54.000	24.000	195.800	196.600	196.300	196.700	196.500	196.800
11.000	15.000	54.000	33.000	195.800	196.600	196.400	196.700	196.500	196.[illegible]
11.000	15.000	54.000	41.000	195.800	196.600	196.300	196.700	196.500	196.800
11.000	15.000	54.000	49.000	195.800	196.700	196.400	196.700	196.500	196.800
11.000	15.000	54.000	57.000	195.900	196.600	196.300	196.700	196.400	196.[illegible]
11.000	15.000	55.000	5.000	196.100	196.700	196.300	196.700	196.400	196.800
11.000	15.000	55.000	13.000	196.800	196.800	196.400	196.700	196.400	196.800
11.000	15.000	55.000	21.000	197.900	197.100	196.600	196.800	196.400	196.[illegible]
11.000	15.000	55.000	29.000	199.400	197.600	196.800	196.800	196.400	196.900
11.000	15.000	55.000	38.000	201.300	198.300	197.200	196.900	196.500	196.900
11.000	15.000	55.000	46.000	203.300	199.100	197.800	197.100	196.500	196.[illegible]
11.000	15.000	55.000	54.000	205.500	200.100	198.400	197.400	196.500	196.900
11.000	15.000	56.000	2.000	207.900	201.300	199.200	197.700	196.700	196.[illegible]
11.000	15.000	56.000	10.000	210.200	202.500	200.100	198.100	196.800	197.000
11.000	15.000	56.000	18.000	212.600	203.800	201.000	198.500	196.900	197.000
11.000	15.000	56.000	26.000	215.000	205.300	202.100	199.100	197.200	197.100
0.000	0.000	0.000	0.000	0.000	0.000	0.000	0.000	0.000	0.000
0.000	0.000	0.000	0.000	0.000	0.000	0.000	0.000	0.000	0.000
0.000	0.000	0.000	0.000	0.000	0.000	0.000	0.000	0.000	0.000
0.000	0.000	0.000	0.000	0.000	0.000	0.000	0.000	0.000	0.000
0.000	0.000	0.000	0.000	0.000	0.000	0.000	0.000	0.000	0.000
0.000	0.000	0.000	0.000	0.000	0.000	0.000	0.000	0.000	0.000
0.000	0.000	0.000	0.000	0.000	0.000	0.000	0.000	0.000	0.000

Explanation of Tables C1 and C2

The first line of each table is a dummy record and is ignored. Each subsequent line of 10 items is a single record, broken down as follows (using the second line of Table C1 as an example):

Item #	Explanation	Value
1-4	day (of month), hour, minute, second	1302:51 hrs, 28 February 1983
5-10	temperature of the six sample thermocouples, ordered outwards from the center	

References

Abey, A. E., W. B. Durham, D. A. Trimmer, and L. L. Dibley (1982), "An Apparatus for Determining the Thermal Properties of Large Geological Samples at Pressures to 0.2 GPa and at Temperatures to 750 K," *Rev. Sci. Instrum.* **53**, 876–879.

Acton, R. U. (1978), "Thermal Conductivity of S.E. New Mexico Rock Salt and Anhydrite," *Thermal Conductivity 15* (Proc. 15th Int. Conf. Thermal Conductivity), V. V. Mirkovich, Ed. (Plenum Press, New York, NY), pp. 263–276.

Bevington, P. R. (1969), *Data Reduction and Error Analysis for the Physical Sciences* (McGraw-Hill, New York, NY), p. 121.

Bridgman, P. W. (1952), *The Physics of High Pressure* (G. Bill and Sons, London), pp. 320–329.

Carter, N. L. and H. C. Heard (1970), "Temperature and Rate Dependent Deformation of Halite," *Am. J. Sci.* **269**, 193–249.

Carter, N. L. and F. D. Hansen (1980), *Mechanical Behavior of Avery Island Halite: A Preliminary Analysis*, prepared for Office of Nuclear Waste Isolation, ONWI-100, and Battelle Memorial Institute, Columbus, OH.

Dixon, M. L. (1982), *Petrographic Report: Insoluble Residue Analysis Permian Cycle 4 Salt Well G. Friemel #1 Palo Duro Basin, Texas*, prepared for Battelle Memorial Institute, Columbus, OH, and the U.S. Department of Energy National Waste Terminal Storage Program.

Durham, W. B., A. E. Abey, and D. A. Trimmer (1981), *Thermal Properties of Avery Island Rock Salt to 573 K and 50 MPa Confining Pressure*, Lawrence Livermore National Laboratory, Livermore, CA, UCRL-53128.

Durham, W. B. and A. E. Abey (1983), "Thermal Conductivity and Diffusivity of Climax Stock Quartz Monzonite at High Pressure and Temperature," *Thermal Conductivity 17* (Proc. 17th Int. Conf. Thermal Conductivity), J. Hust, Ed. (Plenum Press, New York, NY), pp. 459–468.

Edwards, A. L. (1972), *TRUMP: A Computer Program for Transient and Steady-State Temperature Distributions in Multidimensional Systems*, Lawrence Livermore National Laboratory, Livermore, CA, UCRL-14754.

Flieger, H. W. (1963), "The Thermal Diffusivity of Pyroceram at High Temperatures," *Proc. 3rd Conf. Thermal Conductivity* (Oak Ridge National Laboratory, Oak Ridge, TN), (Gatlinburg, TN, Oct. 16–18, 1963) vol. II, pp. 769–783.

Flynn, D. R., H. E. Robinson, and I. L. Martz (1964), "Present Status of Pyroceram Code 9606 as a Thermal Conductivity Reference Standard," *Proc. 4th Conf. Thermal Conductivity* (U.S. Naval Radiological Defense Laboratory, San Francisco, CA, Oct. 13–16, 1964), pp. I-F-1 to I-F-27.

Fujisawa, H., N. Fujii, H. Mizutani, H. Kanamori, and S. Akimoto (1968), "Thermal Diffusivity of Mg_2SiO_4, Fe_2SiO_4, and NaCl at High Pressures and Temperatures," *J. Geophys. Res.* **73**, 4733.

Fukui, L. M. (1982), *Petrographic Report: Insoluble Residue Analysis Permian Cycle 5 Salt G. Friemel #1 and Detten #1 Wells Palo Duro Basin, Texas*, prepared for Battelle Memorial Institute, Columbus, OH, and the U.S. Department of Energy National Waste Terminal Storage Program.

Kieffer, S. W., J. C. Getting, and G. C. Kennedy (1976), "Experimental Determination of the Pressure Dependence of the Thermal Diffusivity of Teflon, Sodium Chloride, Quartz, and Silica," *J. Geophys. Res.* **81**, 3018–3024.

Mirkovich, V. V., W. B. Durham, and H. C. Heard (1983), "Measurement of Thermal Diffusivity of Rocks at High Pressure," *Proc. 8th European Conf. Thermophysical Properties* (Baden-Baden, Federal Republic of Germany, 1982), pp. 255–264.

Morgan, M. T. (1979), *Thermal Conductivity of Rock Salt from Louisiana Salt Domes*, Oak Ridge National Laboratory, Oak Ridge, TN, ORNL/TM-6809.

Plummer, W. A., D. E. Campbell, and A. A. Comstock (1962), "Method of Measurement of Thermal Diffusivity to 1000°C, *J. Am. Cer. Soc.* **45**, 310–316.

Ruskin, R. L. (1963), *Thermal Diffusivity Measurements on Metals and Ceramics at High Temperatures*, Office of Technical Services, U.S. Dept. of Commerce, Washington, D.C., Technical Documentary Report No. ASD-TDR-62-24, part II.

Schneider, P. J. (1955), *Conduction Heat Transfer* (Addison-Wesley, Reading, MA), ch. 1.

Sutherland, H. J. and S. P. Cave (1980), "Argon Gas Permeability of New Mexico Rock Salt under Hydrostatic Compression," *Int. J. Rock Mech. Min. Sci.* **17**, 281–288.

Touloukian, Y. S., R. W. Powell, C. Y. Ho, and P. G. Klemens (1970), *Thermophysical Properties of Matter*, vol. 2, IFI of *Thermal Conductivity Non Metallic Solids* (Plenum Press, New York, NY) p. 942.

Touloukian, Y. S. and C. Y. Ho., Eds. (1981), *Physical Properties of Rocks and Minerals*, McGraw-Hill/CINDAS Data Series on Material Properties (McGraw-Hill, New York, NY), vol. II-2, ch. 12.

Walsh, J. B. and E. R. Decker (1966), "Effect of Pressure and Saturating Fluid on the Thermal Conductivity of Compact Rock," *J. Geophys. Res.* **71**, 3053–3061.

Wawersik, W. and D. W. Hannum (1980), "Mechanical Behavior of New Mexico Rock Salt in Triaxial Compression up to 200°C," *J. Geophys. Res.* **85**, 891–900.

Yang, J. M. (1981), "Thermophysical Properties," in *Handbook of Rock Salt Properties Data*, L. H. Gevantman, Ed., National Bureau of Standards Monograph 167 (U. S. Government Printing Office, Washington, D.C.) ch. 4.

Yukutake, H. and M. Shimada (1978), "Thermal Conductivity of NaCl, MgO, Coesite and Stishovite up to 40 kbar," *Phys. Earth Planet. Interiors* **17**, 193–200.

GLE/km/sb